NASA Technical Paper 1261

Procedures for Generation and Reduction of Linear Models of a Turbofan Engine

Kurt Seldner and David S. Cwynar

AUGUST 1978

NASA

NASA Technical Paper 1261

Procedures for Generation and Reduction of Linear Models of a Turbofan Engine

Kurt Seldner and David S. Cwynar
Lewis Research Center
Cleveland, Ohio

National Aeronautics
and Space Administration

**Scientific and Technical
Information Office**

1978

PROCEDURES FOR GENERATION AND REDUCTION OF LINEAR MODELS OF A TURBOFAN ENGINE

by Kurt Seldner and David S. Cwynar

Lewis Research Center

SUMMARY

A real-time hybrid simulation of the Pratt & Whitney F100-PW-F100 turbofan engine was used for linear-model generation. The linear models were used to analyze the effect of disturbances about an operating point on the dynamic performance of the engine. A procedure that disturbs, samples, and records the state and control variables was developed.

For large systems, such as the F100 engine, the state vector is large and may contain high-frequency information not required for control. Thus, reducing the full-state to a reduced-order model may be a practicable approach to simplifying the control design. A reduction technique was developed to generate reduced-order models. Selected linear and nonlinear output responses to exhaust-nozzle area and main-burner-fuel-flow disturbances are presented for comparison.

INTRODUCTION

During the past decade linear-control-design techniques for multiple-input - multiple-output (multivariable) systems have been the subject of much research. Most require a linear time domain or state-space formulation of the dynamic characteristics of the process. Although modern turbofan and turbojet engines are considered multivariable processes, they are normally described by many nonlinear, dynamic relations. Thus, linearization procedures must be used to obtain a linear, state-space representation of the nonlinear, multivariable process. Because the linear models are only valid about a particular operating point, several models must be generated to describe the engine operation over a wide operating envelope. Once linear models are obtained, the control can be designed using a linear multivariable procedure.

Digital and hybrid engine simulations are available to extract linear models at various operating points throughout the flight envelope. This report describes the pro-

cedure for extracting linear models from a real-time hybrid computer simulation of a turbofan engine - the Pratt & Whitney F100-PW-100(3) engine (ref. 1). The computer simulation was developed as part of the F100 multivariable-control, synthesis program, sponsored jointly by the Air Force Aeropropulsion Laboratory and the NASA Lewis Research Center.

The report includes (1) a description of the engine simulation, (2) a brief description of the analytical basis for the linear-model generation technique, (3) a method for reducing the resultant linear-model complexity by eliminating unwanted information, and (4) a presentation of selected dynamic responses for both nonlinear and linear models. The hybrid-computer listings for generating the disturbance data for computing linear models, system matrices, and eigenvalues for several operating conditions are presented in the appendix.

DESCRIPTION OF F100 TURBOFAN ENGINE

The Pratt & Whitney F100-PW-100(3) engine (fig. 1) is an axial, mixed-flow, twin-spool, low-bypass-ratio turbofan with afterburning capability. The engine has a single inlet for both fan and core airflow. The fan airflow is separated into two streams: one passing through the fan duct and the other passing through the engine core. A three-stage fan is connected to a two-stage, low-pressure turbine. A 10-stage compressor is connected through a hollow shaft to a two-stage high-pressure turbine. The fan has variable guide vanes; the compressor has a variable guide vane followed by two variable rear stator vanes. Compressor discharge bleed air is used for cooling the high- and low-pressure turbine blades and for powering the augmentor turbopump.

The main combustor consists of an annular diffuser with 16 fuel nozzles. The duct and core streams combine in the augmentor section and discharge through a variable convergent-divergent nozzle. The augmentor consists of a diffuser section with five concentric fuel manifolds.

The basic engine-control system consists of a hydromechanical fuel-control system and an electronic-supervisory-control system. The function of the hydromechanical control is to (1) meter fuel to the main burner as a function of power-lever angle (PLA), compressor speed N_H, fan-discharge total pressure P_{13}, and compressor-discharge-static pressure P_{S3}, (2) position the compressor-stator vanes to improve starting and high Mach number characteristics, (3) meter fuel to the five afterburning zones as a function of power-lever angle, fan-duct discharge temperature, and compressor-discharge-static pressure, and (4) control exhaust-nozzle area to maintain desired engine airflow during augmented operation.

The electronic supervisory-control positions the inlet-guide vanes, trims main-combustor-fuel flow to maintain engine operation within safe limits, and trims exhaust-

nozzle area to satisfy engine-flow requirements (refs. 1 and 2).

ENGINE SIMULATION

The development and evaluation of controls for aircraft propulsion systems requires a dynamic model of the engine and control system. The simulation allows us to study and predict engine performance over the specified operating range. The mathematical model can also be used to evaluate various control concepts and to study problems during the development and testing phases of an engine.

The details of a hybrid-computer simulation for the P&W F100-100(3) turbofan engine are reported in reference 1. The engine was modeled in real time on the EAI 680-640 hybrid computer. Real-time simulation permits operation with digital control software. Figure 2 is a block diagram of the interconnection of the various engine components as well as their significant variables. The real-time, hybrid-computer, engine simulation was modeled according to the engine manufacturer's digital simulation. The steady-state characteristics of the rotating elements (compressor, fan and turbine performance maps) were extracted from this digital simulation. The digital portion of the hybrid computer was used to generate nonlinear bivariate functions for the component performance maps. Interconnecting volumes between components were used whenever the gas dynamics are significant or are required to prevent computer instability due to algebraic loops. The continuity, energy, and state equations were solved for each volume. The equations for conservation of angular momentum are used for the fan- and compressor-speed calculations.

LINEAR MODEL GENERATION

Linearization of Model

The F100 engine is a complex, nonlinear, dynamic process consisting of many states. Small-signal-linearization techniques (ref. 3) can be used to represent the nonlinear process about an operating point by a set of first-order matrix differential equations. The system equations can be written as

$$\dot{x} = Ax + Bu \tag{1}$$

$$y = Cx + Du \tag{2}$$

$$z = Hx \tag{2a}$$

Equation (1) defines the relation between the system states X_i ($i = 1, 2, \ldots, n$) and the forcing function u_j ($j = 1, 2, \ldots, p$). Equation (2) relates the outputs y to the states X_i and control inputs u_j. The symbols are defined in appendix A.

Linear models generated from the real-time, hybrid-computer, engine simulation contain all states defined by the engine model. The states as well as control and output variables are as follows:

Engine state variables:

(1) Fan speed, N_L, rpm
(2) Compressor speed, N_H, rpm
(3) High-turbine-inlet pressure, P_4, N/cm^2
(4) Stored mass in the fan-turbine-inlet volume, W_{41}, kg
(5) Nozzle-inlet pressure, P_7, N/cm^2
(6) Fan-turbine-inlet pressure, P_{41}, N/cm^2
(7) Stored mass in the fan duct, W_{13}, kg
(8) Fan-duct temperature, T_{13}, K
(9) Stored mass in the high-turbine-inlet volume, W_4, kg
(10) Stored mass in the compressor-discharge volume, W_3, kg
(11) Compressor-discharge temperature, T_3, K
(12) Afterburner-inlet pressure, P_6, N/cm^2
(13) Stored mass in the afterburner-inlet volume, W_6, kg
(14) Stored mass in the nozzle-inlet volume, W_7, kg
(15) Afterburner gas flow, $\dot{w}_6$, kg/sec
(16) Fan-duct airflow, $\dot{w}_{13}$, kg/sec

Control variables:

(1) Fan-inlet-guide-vane angle, CIVV, deg
(2) Rear compressor variable vanes angle, RCVV, deg
(3) Nozzle throat area, A_n, m^2
(4) Main-burner-fuel flow, $\dot{w}_{f4}$, kg/hr
(5) Afterburner fuel flow, $\dot{w}_{f7}$, kg/hr

Output variables:

(1) Fan airflow, $\dot{w}_{fan}$, kg/sec
(2) Rear compressor-variable-vane angle, RCVV, deg
(3) Net thrust, F_n, kN
(4) High-turbine-inlet temperature, T_4, K
(5) Fan-discharge-flow parameter, $\Delta P/P_{13}$
(6) Fan sall margin, SMF
(7) High-compressor-stall margin, SMHC

Linear models must be generated about an operating point along the normal operating line of the engine. Since these models only describe the engine performance for small input disturbances at a specified operating point, several linear models must be generated. The process of disturbing, sampling, recording, and reducing the raw data is automated. Disturbances of state and control variables are used to generate data from which the various elements of the system matrices of equations (1) and (2) can be determined. The magnitude of the disturbance is limited to ±2 percent to insure that performance is maintained within a linear range of operation. The resulting linear models describe the dynamic performance of the engine about the specified operating point.

Linear Model Generation

The process of acquiring the data for model generation is outlined in figure 3. To generate linear-state models, the engine simulation must be set up at a specified power and flight condition. At the desired operating condition a hybrid subroutine (STATE 1) can be used to set the initial conditions for the desired operating condition. After the initial conditions (steady-state values for state variables) are set, the analog portion of the hybrid computer can now be placed in the "initial condition" mode. This procedure prevents integrator drift during the sampling and data recording process. Another hybrid subroutine (STATE 2) applies the disturbances to the state and control variables. The disturbance data are trunked to the SEL810B digital computer for sampling and recording. The two subprogram listings (STATE 1 and STATE 2) are given in appendix B.

The block diagram in the lower portion of figure 3 illustrates the sampling, verifying, and recording processes of the disturbance data. The processes are outlined in more detail in the flow charts of figure 4. On initiation of the sampling process, a time-delay circuit is activated to insure that the simulation is steady state. A latch circuit is also set to $L = -2$ and updated during the process for logical decisions. Each engine variable was sampled 4096 times, and a mean M_1 was calculated for each variable. The sampling process was repeated, and a second mean M_2 was calculated. The two means M_1 and M_2 were compared. If the error between the means is within 5 millivolts, the data are accepted and descaled to engineering units. If the error between M_1 and M_2 exceeds 5 millivolts, the sampling and validation process is repeated. At this time the latch circuitry is also updated. If the M_1 and M_2 are not within tolerance after the second trial, the process is terminated and the operator alerted. All acceptable data are stored on a floppy disk before being transmitted to the IBM 360 computer.

The sampled data must be read into the IBM 360 computer. Figure 5 presents a block diagram showing the data verification, processing, and linear model generation. After the sampled, descaled data are read into the computer, the mantissa and characteristic of each variable are added to form a check-sum. The check-sum value is

compared with that stored on the floppy disk by the SEL810B computer. If the two values agree, the process continues to the validation mode. If the two values do not agree, the process is terminated, and the data must be corrected.

The data were then validated by verifying that the correct variables were disturbed and that the removal of the disturbance resets the state and control variables. A base run (without disturbances) was used for comparison. The tolerance between the two sets of data (base and reset) must be within a specified tolerance. If they are within tolerance, the data can be processed to compute the system matrices. The matrix computations used both positive and negative disturbances to obtain a better average and minimize numerical errors. The system matrices were stored in the IBM 360 computer for later use in calculating the dynamic characteristics of the linear models.

LINEAR MODEL OPERATIONS

State Vector Transformation

Some of the states generated by the F100, real-time simulation, such as mass, may not be measurable and must be converted to either a pressure or temperature relation. Taylor's series and the equation of state were used to modify the state vector so that it included only desirable measurements for the linear models. These generated models are valid only for small disturbances about a steady-state operating point. The mathematical analysis relating the linear transformation of the state vector is as follows: Expand Taylor's series about the nominal operating conditions P_0, T_0, W_0, where these values are the steady-state conditions at the engine-operating point. The Taylor-series expansion for temperature T about the nominal steady-state point T_0 becomes:

$$(T - T_0) = \left.\frac{\partial T}{\partial P}\right|_{\substack{P=P_0\\W=W_0}} (P - P_0) + \left.\frac{\partial T}{\partial W}\right|_{\substack{P=P_0\\W=W_0}} (W - W_0) + \frac{1}{2!}\left[\left.\frac{\partial^2 T}{\partial P^2}\right|_{\substack{P=P_0\\W=W_0}} (P - P_0)^2 + 2\left.\frac{\partial^2 T}{\partial P\,\partial W}\right|_{\substack{P=P_0\\W=W_0}} (P - P_0)(W - W_0) + \left.\frac{\partial^2 T}{\partial W^2}\right|_{\substack{P=P_0\\W=W_0}} (W - W_0)^2\right] + \text{higher order terms (HOT)} \tag{3}$$

The equation of state is

$$P = \frac{R_A}{V} WT \tag{4}$$

where R_A is the gas constant of air (in N · cm/kg · K) and V is the volume (in cm^3). We may rewrite equation (4) so that

$$T = \frac{V}{R_A} \frac{P}{W} \tag{4a}$$

Differentiating equation (4a) yields

$$\frac{\partial T}{\partial P} = \frac{V}{R_A W} \qquad \frac{\partial T}{\partial W} = -\frac{V}{R_A} \frac{P}{W^2} \qquad \frac{\partial^2 T}{\partial P \, \partial W} = -\frac{V}{R_A W^2}$$

$$\frac{\partial^2 T}{\partial P^2} = 0 \qquad \frac{\partial^2 T}{\partial W^2} = 2 \frac{V}{R_A} \frac{P}{W^3}$$

And substituting into equation (3) yields

$$(T - T_0) = \frac{V}{R_A W} (P - P_0) - \frac{VP}{R_A W^2} (W - W_0)$$

$$- \frac{V}{R_A W^2} (P - P_0)(W - W_0) + \frac{VP}{R_A W^3} (W - W_0)^2 + HOT \tag{5}$$

If we neglect second- and higher-order terms, equation (5) becomes

$$(T - T_0) = \frac{V}{R_A W} (P - P_0) - \frac{VP}{R_A W^2} (W - W_0) \tag{6}$$

If

$$K = \frac{V}{R_A} \qquad \Delta T = (T - T_0) \qquad \Delta P = (P - P_0) \qquad \Delta W = (W - W_0)$$

then, equation (6) reduces to

$$\Delta T = \frac{K}{W} \Delta P - \frac{KP}{W^2} \Delta W \tag{7}$$

Differentiating equation (3) yields

$$\dot{\overline{\Delta T}} = \frac{\partial T}{\partial P} \dot{\overline{\Delta P}} + \frac{\partial T}{\partial W} \dot{\overline{\Delta W}} + \frac{\partial^2 T}{\partial P^2} \overline{\Delta P} \cdot \dot{\overline{\Delta P}} + \frac{\partial^2 T}{\partial P \, \partial W} \dot{\overline{\Delta P}} \, \Delta W$$

$$+ \frac{\partial^2 T}{\partial P \, \partial W} \overline{\Delta P} \, \dot{\overline{\Delta W}} + \frac{\partial^2 T}{\partial W^2} \overline{\Delta W} \, \dot{\overline{\Delta W}} + HOT \tag{8}$$

When all second-order and higher-order terms are neglected, equation (8) reduces to

$$\dot{\overline{\Delta T}} = \frac{\partial T}{\partial P} \dot{\overline{\Delta P}} + \frac{\partial T}{\partial W} \dot{\overline{\Delta W}} \tag{9}$$

Substituting for the partial derivatives yields

$$\dot{\overline{\Delta T}} = \frac{K}{W} \dot{\overline{\Delta P}} - \frac{KP}{W^2} \dot{\overline{\Delta W}} \tag{10}$$

Similarly, for $\dot{\overline{\Delta P}}$

$$\dot{\overline{\Delta P}} = \frac{\partial P}{\partial T} \dot{\overline{\Delta T}} + \frac{\partial P}{\partial W} \dot{\overline{\Delta W}} \tag{11}$$

or

$$\dot{\overline{\Delta P}} = \frac{W}{K} \dot{\overline{\Delta T}} + \frac{T}{K} \dot{\overline{\Delta W}} \tag{12}$$

Using equations (10) and (12) allows the state vector to be transformed to include only pressure, temperature, and flow relations. The transformation of the state vector can be achieved through a transformation matrix E that relates pressure and temperature to mass in the volume. In matrix form

$$X_1 = Ex \tag{13}$$

where X is the original state vector, X_1 is the transformed state vector, and E is the transformation matrix. Substituting equation (13) into equations (1), (2), and (2a) and simplifying yield

$$\dot{X}_1 = \bar{A}X_1 + \bar{B}u \tag{14}$$

$$y = \bar{C}X_1 + Du \tag{15}$$

$$z = HX_1 \tag{16}$$

where

$$\bar{A} = EAE^{-1} \qquad n \times n$$

$$\bar{B} = EB \qquad n \times p$$

$$\bar{C} = CE^{-1} \qquad r \times n$$

and where A, B, and C are the original state, control, and output matrices.

Equations (14) to (16) are linear models composed of measurable states. The transformation is a similarity transformation so that the original set of eigenvalues will be retained. The transformation matrix E, of course, varies with engine operating condition; H is the identity matrix since the state vector X_1 contains the transformed states.

Model-Order Reduction

Before reducing the order of the linear model, it may be necessary to permute the state vector so as to group slowly and rapidly decaying states separately. Permutation of the state vector may also be used to select particular states for the lower order models. A similarity transformation can be used to perform this procedure: Let

$$X_2 = E_p X_1 \tag{17}$$

where X_1 is the transformed state vector, X_2 is the permuted state vector, and E_p is the permutation matrix. Substituting equation (17) for state vector X_1 in equations

(14) to (16) yields the permuted linear model:

$$\dot{X}_2 = \bar{A}_n X_2 + B_n u \tag{18}$$

$$y = \bar{C}_n X_2 + Du \tag{19}$$

$$z = H_n X_2 \tag{20}$$

where

$$\bar{A}_n = E_p \bar{A} E_p^{-1} \qquad n \times n$$

$$\bar{B}_n = E_p \bar{B} \qquad n \times p$$

$$\bar{C}_n = \bar{C} E_p^{-1} \qquad r \times n$$

$$H_n = H E_p^{-1} \qquad n \times n$$

and where $\bar{A}$, $\bar{B}$, and $\bar{C}$ are the transformed state, control, and output matrices. Equations (18) to (20) form the linear model for a reordered state vector. If permutation of the state vector is not desired, the resulting matrix E_p is the identity matrix. The output matrices HE_p^{-1} and CE_p^{-1} transform the permuted state vector to the original state output and output vectors. This procedure is required to maintain the original order of the outputs for data identification and plotting.

The selection of an appropriate set of states for the reduced model is the problem imposed by linear model reduction. Model-order reduction can be based on the principle that the state vector can be permuted into separate groups of slowly and rapidly decaying states. (Usually a 10:1 separation between eigenvalues can be considered as acceptable.) However, the eigenvalues in most physical systems, cannot be readily separated, and the identification of states with specific eigenvalues is a difficult, if not impossible, task. In addition, specific states must be included in the reduced-order-linear-model representation. Therefore, the reduced-order-linear-model state vector must be based on intuition and turbofan-engine controls experience. The states that should be considered are those required by the engine controller and protective devices.

The state vector must be partitioned into two state vectors: one with the desired states for the reduced-order model, and the second with the remaining states that will be eliminated. The dynamic characteristics of the latter states are neglected by setting the derivatives to zero. These states are approximated by their steady-state values.

The eliminated states are then reconstructed from information contained in the reduced-order model. The reduction technique is described in references 4 to 6. The mathematical formulation is as follows:

$$X_s = \frac{X_{s1}}{X_{s2}} \tag{21}$$

where X_{s1} is state vector of retained system states and X_{s2} is the state vector of eliminated system states. Applying the notation of equation (21) to equation (1) yields

$$\begin{pmatrix} \dot{X}_{s1} \\ \hdashline \dot{X}_{s2} \end{pmatrix} = \left(\begin{array}{c:c} A_{11} & A_{12} \\ \hdashline A_{21} & A_{22} \end{array}\right)\begin{pmatrix} X_{s1} \\ \hdashline X_{s2} \end{pmatrix} + \begin{pmatrix} B_1 \\ \hdashline B_2 \end{pmatrix} u \tag{22}$$

where A_{11}, A_{12}, A_{21}, A_{22}, B_1, and B_2 are matrices resulting from the partitioning of the $n \times 1$ state vector X_s. The solution of equation (22) for $\dot{X}_{s1}$ and $\dot{X}_{s2}$ is

$$\left.\begin{aligned} \dot{X}_{s1} &= A_{11}X_{s1} + A_{12}X_{s2} + B_1 u \\ \dot{X}_{s2} &= A_{21}X_{s1} + A_{22}X_{s2} + B_2 u \end{aligned}\right\} \tag{23}$$

By setting $\dot{X}_{s2} = 0$ and substituting into the $\dot{X}_{s1}$ relation

$$X_{s2} = -A_{22}^{-1}(A_{21}X_{s1} + B_2 u) \tag{24}$$

the $\dot{X}_{s1}$ relation becomes

$$\dot{X}_{s1} = \left(A_{11} - A_{12}A_{22}^{-1}A_{21}\right)X_{s1} + \left(B_1 - A_{12}A_{22}^{-1}B_2\right)u \tag{25}$$

For the output equation (2)

$$y = \left(C_1 \,\vdots\, C_2\right)\begin{pmatrix} X_{s1} \\ \hdashline X_{s2} \end{pmatrix} + Du \tag{26}$$

where C_1 and C_2 are matrices resulting from the partitioning of the output vector y. Substituting for X_{s2} in equation (26) yields

$$y = \left(C_1 - C_2A_{22}^{-1}A_{21}\right)X_{s1} + \left(D - C_2A_{22}^{-1}B_2\right)u \tag{27}$$

Similarly, for equation (2a)

$$z = \left(H_1 - H_2A_{22}^{-1}A_{21}\right)X_{s1} - H_2A_{22}^{-1}B_2u \tag{28}$$

where H_1 and H_2 are matrices resulting from the partitioning of the state output vector z. The dimensions of the state, control, and output vectors, and system matrices are given in appendix A. Rewriting equations (25), (27), and (28) yields

$$\begin{aligned} \dot{X}_{s1} &= \overline{A}_sX_{s1} + \overline{B}_su \\ y &= \overline{C}_sX_{s1} + \overline{D}_su \\ z &= \overline{H}_sX_{s1} + \overline{H}_uu \end{aligned} \tag{29}$$

where

$$\overline{A}_s = \left(A_{11} - A_{12}A_{22}^{-1}A_{21}\right)$$

$$\overline{B}_s = \left(B_1 - A_{12}A_{22}^{-1}B_2\right)$$

$$\overline{C}_s = \left(C_1 - C_2A_{22}^{-1}A_{21}\right)$$

$$\overline{D}_s = \left(D - C_2A_{22}^{-1}B_2\right)$$

$$\overline{H}_s = \left(H_1 - H_2A_{22}^{-1}A_{21}\right)$$

$$\overline{H}_u = -H_2A_{22}^{-1}B_2$$

Equations (29) represent the reduced-order-linear model. The system matrices (A, B, C, D, H) must be replaced by the reduced-order linear model matrices ($\overline{A}_s$, $\overline{B}_s$, $\overline{C}_s$, $\overline{D}_s$, $\overline{H}_s$). The reduced-order model matrices contain sufficient information to reconstruct all eliminated states and outputs. It should be emphasized that the reduced-model accuracy is strongly dependent on the eigenvalues for the retained and eliminated states. If the ratio of the lowest eigenvalue for the eliminated states to the highest

eigenvalue for the retained states is large, a good approximation to the full-state linear model can be achieved. A property of the normal reduction technique is that the condition $\dot{X}_{s2} = 0$ forces the final value of the reduced models to the same steady-state value. This type of reduction is known as a type II method. An alternative method whereby $X_2 = 0$ is identified as a type I reduction technique.

The real-time, hybrid computer simulation of the Pratt & Whitney F100-PW-100(3) turbofan engine was used to determine the linear models at the sea-level-static condition. The state, control, and output matrices of equations (1) and (2) were generated at several power conditions along the operating line. The system matrices for the linear model representation are presented in appendix C.

The state and control disturbances were limited to insure that engine performance would be maintained over its linear operating range. Because of the low-level disturbance signals, the output variations were so small that they caused large errors in the sampling process. The errors are mainly due to resolution and inaccuracies of the recording devices. Studies can be conducted to establish the optimum magnitudes of the disturbance signals to obtain good correlation between nonlinear and linear models. However, because of the tremendous effort expended in generating system matrices, the magnitudes of the disturbances were maintained at a constant value. The model-reduction technique, described previously, was used to reduce the full-state (16th order) linear models to lower-order models. The system matrices for several reduced-order models at the sea-level-static intermediate power condition are given in appendix C.

DISCUSSION OF RESULTS

Nonlinear and Full-State Models

Figures 6 and 7 present the comparison of nonlinear and full-state-linear-model responses to step changes in exhaust-nozzle area and main-burner-fuel flow. The nonlinear responses were obtained from the F100-PW-100(3) real-time hybrid computer simulation.

Figure 6(a) presents the change in fan speed N_L to a step change in exhaust-nozzle area. The two responses are at first quite close, but a slightly lower final steady-state value is obtained for the nonlinear model response. This error is about 12 rpm or 11 percent. Similar responses for compressor speed N_H are shown in figure 6(b). The linear and nonlinear models exhibit different performance characteristics in that the final value of the linear model is much smaller than the nonlinear. The dynamic difference between the nonlinear and linear models is caused by low signal levels. The accuracy and resolution of the analog-digital converters may be insufficient to detect the low signal levels. The results for fan turbine-inlet temperature T_{41} are given in

figure 6(c). The nonlinear and linear models exhibit similar characteristics. The nonlinear model experiences a higher temperature overshoot (about 1 K) than the full-state model. The final value of the nonlinear response is slightly lower (about 2.2 K). The extremely small magnitude of the final value (0.15 mV) for the full-state response is causing inaccurate results. The responses illustrating the change in exhaust-nozzle pressure P_7 for a change in exhaust-nozzle area are shown in figure 6(d). The characteristics of the two models follow closely with a final steady-state error of about 0.028 N/cm^2 or 6.6 percent. Thrust responses are shown in figure 6(e). Thrust is an output quantity so that the feed-forward term Du contributes to the initial thrust. The feed-forward matrix D represents the direct, linear relation between output y and input u. Slightly more undershoot can be noted for the nonlinear response. The final steady-state error is about 0.17 kN.

Figure 7 presents selected step responses to fuel-flow disturbances in the main burner. The change in fan speed N_L is given in figure 7(a). Although the nonlinear and linear models exhibit similar dynamic characteristics, a steady-state error of 11 rpm, or 15.9 percent, was obtained. The responses for compressor speed N_H are compared in figure 7(b). The two models exhibit similar characteristics, although a final steady-state error of 15 rpm, or 30 percent, was observed. The magnitude of the signal levels for the full-state model is small (about 2.4 mV max) causing large errors. The accuracy of the analog digital converters is evident for the full state response. The results for main burner pressure P_4 for a fuel-flow disturbance are presented in figure 7(c). The nonlinear response exhibits the same trend as the linear response; however, a final steady-state error of 0.5 N/cm^2 or 17 percent was noted. The responses for fan turbine-inlet temperature T_{41} are shown in figure 7(d). The nonlinear response shows slightly more temperature overshoot and a 0.8 K or 10 percent higher steady-state value than the linear response. The change in exhaust-nozzle pressure to a fuel-flow disturbance is presented in figure 7(e). Although the nonlinear response follows the same trend as the linear model; it had a final steady-state error of 0.035 N/cm^2, or 14 percent. The change in thrust is given in figure 7(f). A higher final steady-state value (about 0.13 kN or 15 percent) was obtained for the nonlinear response.

Full-State and Reduced-Order Models

The responses for full-state and reduced-order linear models for step changes in exhaust-nozzle area and main-burner-fuel flow are presented in figures 8 and 9. Step responses for several reduced-order models were generated to establish the model order that would most closely match the full-state model. The adequacy of the full-state and reduced-order linear models to describe the nonlinear engine was determined by applying disturbances (area and fuel flow) to the various linear models and observing

the transient behavior.

The change in fan speed N_L to a step change in exhaust-nozzle area for several linear models is presented in figure 8(a). Excellent agreement was obtained for the full-state and seventh-order linear models. A slightly faster rise time can be observed for the lower order models (fifth and third). The dynamics of the linear models are nearly identical, and fan speed could be approximated by a lower order model. Similar step responses for compressor speed are shown in figure 8(b). Excellent agreement can be observed between the full-state and seventh-order models. A slightly faster rise time was noted for the fifth- and third-order models. The response characteristics of the linear models differ from the nonlinear model (fig. 6(b)). As mentioned previously, the results for the linear models may contain inaccuracies due to the signal levels being too low for accurate detection by the conversion devices. Again, the full-state model can be approximated by a lower order model. The results for burner pressure P_4 (fig. 8(c)) show extremely small burner-pressure variations for a step change in exhaust-nozzle area. Excellent agreement can be observed for the full-state and seventh-order models and for the fifth- and third-order models. A slightly larger pressure undershoot exists for the two lower order models. The responses for fan-turbine-inlet temperature T_{41} are given in (fig. 8(d)). This state is a reconstructed quantity for the third-order model, as is evident from the initial temperature rise. The feed-forward term $\overline{H}_u$ in the state output equation (29) contributes to the initial temperature rise. The magnitude of the signal levels (about 0.5 mV) is extremely small and can cause difficulties in the sampling process. The responses illustrating the change in exhaust-nozzle pressure P_7 for an exhaust nozzle disturbance (fig. 8(e)) show excellent agreement between full-state and seventh-order linear models. Since exhaust-nozzle pressure is a reconstructed state for the third-order model, the feed-forward term $\overline{H}_u$ causes an initial pressure drop of 0.59 N/cm^2. After the initial transients, good agreement is obtained between the fifth- and third-order models. The thrust F_N responses are presented in figure 8(f). Because thrust is an output quantity, the feed-forward term Du causes an initial change. The agreement for the full-state and seventh-order model is favorable, but slightly more undershoot is obtained for the full-state model. The third-order model response initially differs from the fifth-order response, but after 25 msec follows closely.

Figures 9 present selected responses to main-burner-fuel-flow disturbances. The change in fan speed N_L results (fig. 9(a)) show excellent agreement between the various linear models. However, the seventh-order model has a slightly higher rise time than the other reduced-order linear models. Since the dynamic characteristics of the full-state and reduced-order models are extremely close, the full-state model can be approximated by a lower order model. Excellent agreement can also be noted in the responses for compressor speed N_H (fig. 9(b)) for the full-state and seventh-order models and the two lower order models. The results for burner pressure P_4 (fig. 9(c)) show that the responses for the various linear models are extremely close and allow the

full-state model to be approximated by a lower order model. Fan-turbine-inlet temperature T_{41} responses are shown in figure 9(d). The temperature overshoot of the reduced order models is slightly higher than the full state model. However, good agreement between the various linear models can be observed. The fan-turbine-inlet temperature is a reconstructed state for the third-order model as indicated by the initial temperature rise. The change in exhaust-nozzle pressure P_7 for a fuel-flow disturbance is given in figure 9(e). Good agreement can be noted for the full-state and seventh-order models. A slightly faster rise time is exhibited by the two lower order models. Since exhaust-nozzle pressure is a reconstructed state for the third-order model, there is a small, initial pressure decrease in the response. The change in thrust F_N is given in figure 9(f). Good agreement can be noted for the full-state and seventh-order models; whereas a slightly faster initial rise time was observed for the fifth- and third-order models.

The eigenvalues for several full-state linear models along the sea-level-static, normal operating line are presented in table I. The eigenvalues for the full-state-linear and selected reduced-order-linear models are tabulated in table II. A graphical representation of the eigenvalues for the full-state and fifth-order models is given in figure 10. This analysis indicates that the important eigenvalues are located at (-4.86, -6.49) and (-4.25, -6.85). Similar results were obtained for the seventh- and third-order reduced models. Without further investigation these results imply that the dynamic characteristics of the full-state model can adequately be represented by a second-order model, such as the two rotor speeds. However, additional system states may be required for engine control and protection.

SUMMARY OF RESULTS

A real-time, hybrid-engine simulation was formulated to evaluate the multivariable-control concept over specified power and flight conditions. The simulation was also used to generate linear models that describe the dynamic performance for low-level control disturbances. The latter task was performed to demonstrate linear-model-generation techniques and develop computer methods for sampling and recording the disturbance data. The linear-model matrices were computed on the IBM 360 computer.

The linear models, valid about a nominal operating point, were used to obtain the response characteristics for exhaust-nozzle area and main-burner-fuel-flow disturbances. The linear models were cross-plotted with the nonlinear responses. Differences in the dynamic responses and final steady-state values can be observed for the linear and nonlinear models. The nonlinear models exhibit, for several conditions, slightly larger overshoot or undershoot. The difficulties encountered in the sampling and recording process are evident by the final value errors. In many cases the signal levels are ex-

tremely small and below the resolution of the analog-digital conversion modules.

For large systems, such as the F100 turbofan engine, the order of the state vector is large and may contain high-frequency information not required for control purposes. Thus, reduction of the full-state model to a reduced, lower order model could be a viable approach to simplifying the control design procedure. A reduction technique was developed to generate reduced-order models.

The comparison indicates good agreement for full-state and seventh-order models. The initial dynamic characteristics of the lower order models differs from the higher order responses. The error can be attributed to the type of reduction and could possibly be minimized by proper state selection for the reduced-order models. The type II reduction method, due to the $\dot{X}_2 = 0$ approximation, forces the final steady-state values to identical magnitudes.

The advantages of the hybrid simulation are the ease and flexibility in setting flight and power conditions of the turbofan engine. However, the accuracy and repeatability accomplished by a digital simulation cannot be matched with the hybrid simulation. As noted by the nonlinear and linear results, errors can be introduced by the low signal and high noise levels. These small signals can also cause errors in the sampling and recording processes.

Lewis Research Center,
National Aeronautics and Space Administration,
Cleveland, Ohio, March 16, 1978,
505-05.

APPENDIX A

SYMBOLS

A	state matrix $n \times n$
$\overline{A}$	transformed state matrix $n \times n$
$\overline{A}_n$	permuted state matrix $n \times n$
$\overline{A}_s$	reduced-order state matrix $m \times m$
A_{11}	partitioned state matrix $m \times m$
A_{12}	partitioned state matrix $m \times (n - m)$
A_{21}	partitioned state matrix $(n - m) \times m$
A_{22}	partitioned state matrix $(n - m) \times (n - m)$
B	control matrix $n \times p$
$\overline{B}$	transformed control matrix $n \times p$
$\overline{B}_n$	permuted control matrix $n \times p$
$\overline{B}_s$	reduced-order control matrix $m \times p$
B_1	partitioned control matrix $m \times p$
B_2	partitioned control matrix $(n - m) \times p$
C	output matrix $r \times n$
$\overline{C}$	transformed output matrix $r \times n$
$\overline{C}_n$	permuted output matrix $r \times n$
$\overline{C}_s$	reduced-order output matrix $r \times m$
C_1	partitioned output matrix $r \times m$
C_2	partitioned output matrix $r \times (n - m)$
D	feed forward matrix $r \times p$
$\overline{D}_s$	reduced-order feed forward matrix $r \times p$
E	state transformation matrix $n \times n$
E_p	state permutation matrix $n \times n$
H	state output matrix $n \times n$
$\overline{H}_n$	permuted state output matrix $n \times n$

$\bar{H}_s$ reduced-order state output matrix $n \times m$

$\bar{H}_u$ reduced-order state feed forward matrix $n \times p$

H_1 partitioned state output matrix $n \times m$

H_2 partitioned state output matrix $n \times (n - m)$

P pressure, N/cm^2

R_A gas constant of air, 2.87×10^4 N · cm/kg K

T temperature, K

u control vector $p \times 1$

V volume, cm^3

W stored mass, kg

X state vector $n \times 1$

X_{s1} state vector (slowly decaying states) $m \times 1$

X_{s2} state vector (rapidly decaying states) $(n - m) \times 1$

X_1 transformed state vector $n \times 1$

X_2 permuted state vector $n \times 1$

APPENDIX B

HYBRID COMPUTER LISTINGS

State Variable Initialization Subroutine (State 1)

```
      SUBROUTINE STATE1(I)
      SCALED FUNCTION VARI(20),I
      DIMENSION AADK(23)
      COMMON/STATE1/VARI,I
      DATA AADK(1),AADK(2),AADK(3),AADK(4),AADK(5),AADK(6),AADK(7),
     1 AADK(8),AADK(9),AADK(10),AADK(11),AADK(12),AADK(13),AADK(14),
     2 AADK(15),AADK(16),AADK(17),AADK(18),AADK(19),AADK(20),AADK(21),
     3 AADK(22),AADK(23)/4HA000,4HA001,4HA002,4HA003,4HA100,4HA101,
     4 4HA085,4HA110,4HA020,4HA111,4HA007,4HA076,4HA000,4HA007,
     5 4HA017,4HA030,4HA001,4HA011,4HA080,4HA076,4HA020,
     6 4HA105,4HA017/
C*****PLACE ANALOGS IN MODE
      CALL OSC(2,IERR)
      CALL OSH(IERR)
C*****READ CONSOLE ONE AMPLIFIERS
      CALL OSC(0,IERR)
      CALL OSC(1,IERR)
      DO 4  I=13,21
      CALL OKAS(AADK(I),VARI(I),IERR)
    4 CONTINUE
C*****READ CONSOLE TWO AMPLIFIERS
      CALL OSC(6,IERR)
      CALL OSC(2,IERR)
      DO 5  I=1,12
      CALL OKAS(AADK(I),VARI(I),IERR)
    5 CONTINUE
      VARI(3)=-VARI(3)
      VARI(5)=-VARI(5)
      VARI(10)=-VARI(10)
      VARI(12)=-VARI(12)
      CALL OKAS(AADK(22),VARI(22),IERR)
      CALL OKAS(AADK(23),VARI(23),IERR)
      VARI(22)=-VARI(22)
      VARI(23)=-VARI(23)
C*****SET IC POTS FOR ALL INTEGRATORS
      CALL OWBDCS(42,VARI(1),16,IERR)
      CALL OWDCS(58,VARI(22),1,IERR)
      CALL OWDCS(71,VARI(23),1,IERR)
C*****PLACE ANALOGS IN IC
      CALL OSC(1,IERR)
      CALL OSIC(IERR)
C*****INITIALIZE FOR STATE2
      L=0
      D=.025
      CALL OSC(0,IERR)
      CALL OSC(1,IERR)
      RETURN
      END
```

State Variable Disturbance Subroutine (State 2)


```
FORTRAN COMPILER REV  LEV  000

      SUBROUTINE STATE2(L)
      SCALED FUNCTION VAR1(2),D,VAR(2)
      COMMON/STATE1/VAR1,D
      CALL USC(6,IERR)
      CALL USC(2,IERR)
 1000 L=L+1
      IF(L.GT.43)  GO TO 47
      IF(L.GT.21)  GO TO 2000
      GO TO (1,2,3,4,5,6,7,8,9,10,11,12,13,14,15,16,17,18,19,20,21),L
 2000 LL=L-21
      GO TO (22,23,24,25,26,27,28,29,30,31,32,33,34,35,36,37,38,39,40,
     1 41,42,43),LL
 3000 FORMAT(3X,12)
C*****NH DISTURBANCE
    1 VAR(1)=VAR1(1)+D*VAR1(1)
      CALL UNDCS(42,VAR(1),1,IERR)
      GO TO 50
    2 VAR(1)=VAR1(1)-D*VAR1(1)
      CALL UNDCS(42,VAR(1),1,IERR)
      GO TO 50
C*****NL DISTURBANCE
    3 VAR(1)=VAR1(1)
      VAR(2)=VAR1(2)+D*VAR1(2)
      CALL UNBDCS(42,VAR(1),2,IERR)
      GO TO 50
    4 VAR(2)=VAR1(2)-D*VAR1(2)
      CALL UNDCS(43,VAR(2),1,IERR)
      GO TO 50
C*****W41 DISTURBANCE
    5 VAR(2)=VAR1(2)
      VAR(3)=VAR1(3)+D*VAR1(3)
      CALL UNBDCS(43,VAR(2),2,IERR)
      GO TO 50
    6 VAR(3)=VAR1(3)-D*VAR1(3)
      CALL UNDCS(44,VAR(3),1,IERR)
      GO TO 50
C*****P7 DISTURBANCE
    7 VAR(3)=VAR1(3)
      VAR(4)=VAR1(4)+D*VAR1(4)
      CALL UNBDCS(44,VAR(3),2,IERR)
      GO TO 50
    8 VAR(4)=VAR1(4)-D*VAR1(4)
      CALL UNDCS(45,VAR(4),1,IERR)
      GO TO 50
C*****P41 DISTURBANCE
    9 VAR(4)=VAR1(4)
      VAR(5)=VAR1(5)+D*VAR1(5)
      CALL UNBDCS(45,VAR(4),2,IERR)
      GO TO 50
   10 VAR(5)=VAR1(5)-D*VAR1(5)
      CALL UNDCS(46,VAR(5),1,IERR)
      GO TO 50
```

```
C*****W6 DISTURBANCE
   11 VAR(5)=VARI(5)
      VAR(6)=VARI(6)+D*VARI(6)
      CALL GWBDCS(46,VAR(5),2,IERR)
      GO TO 50
   12 VAR(6)=VARI(6)-D*VARI(6)
      CALL GWDCS(47,VAR(6),1,IERR)
      GO TO 50
C*****WG6 DISTURBANCE
   13 VAR(6)=VARI(6)
      VAR(7)=VARI(7)+D*VARI(7)
      CALL GWBDCS(47,VAR(6),2,IERR)
      GO TO 50
   14 VAR(7)=VARI(7)-D*VARI(7)
      CALL GWDCS(48,VAR(7),1,IERR)
      GO TO 50
C*****P6 DISTURBANCE
   15 VAR(7)=VARI(7)
      VAR(8)=VARI(8)+D*VARI(8)
      CALL GWBDCS(48,VAR(7),2,IERR)
      GO TO 50
   16 VAR(8)=VARI(8)-D*VARI(8)
      CALL GWDCS(49,VAR(8),1,IERR)
      GO TO 50
C*****W7 DISTURBANCE
   17 VAR(8)=VARI(8)
      VAR(9)=VARI(9)+D*VARI(9)
      CALL GWBDCS(49,VAR(8),2,IERR)
      GO TO 50
   18 VAR(9)=VARI(9)-D*VARI(9)
      CALL GWDCS(50,VAR(9),1,IERR)
      GO TO 50
C*****W12 DISTURBANCE
   19 VAR(9)=VARI(9)
      VAR(10)=VARI(10)+D*VARI(10)
      CALL GWBDCS(50,VAR(9),2,IERR)
      GO TO 50
   20 VAR(10)=VARI(10)-D*VARI(10)
      CALL GWDCS(51,VAR(10),1,IERR)
      GO TO 50
C*****T13 DISTURBANCE
   21 VAR(10)=VARI(10)
      VAR(11)=VARI(11)+D*VARI(11)
      CALL GWBDCS(51,VAR(10),2,IERR)
      GO TO 50
   22 VAR(11)=VARI(11)-D*VARI(11)
      CALL GWDCS(52,VAR(11),1,IERR)
      GO TO 50
C*****WA15 DISTURBANCE
   23 VAR(11)=VARI(11)
      VAR(12)=VARI(12)+D*VARI(12)
      CALL GWBDCS(52,VAR(11),2,IERR)
      GO TO 50
   24 VAR(12)=VARI(12)-D*VARI(12)
      CALL GWDCS(52,VAR(12),1,IERR)
      GO TO 50
C*****W2 DISTURBANCE
   25 VAR(12)=VARI(12)
      VAR(13)=VARI(13)+D*VARI(13)
```

```
      CALL GWBDCS(53,VAR(12),2,IERR)
      GO TO 50
   26 VAR(13)=VAR(13)-D*VAR(13)
      CALL GWDCS(54,VAR(13),1,IERR)
      GO TO 50
C*****T3 DISTURBANCE
   27 VAR(13)=VAR(13)
      VAR(14)=VAR(14)+D*VAR(14)
      CALL GWBDCS(54,VAR(13),2,IERR)
      GO TO 50
   28 VAR(14)=VAR(14)-D*VAR(14)
      CALL GWDCS(55,VAR(14),1,IERR)
      GO TO 50
C*****P4 DISTURBANCE
   29 VAR(14)=VAR(14)
      VAR(15)=VAR(15)+D*VAR(15)
      CALL GWBDCS(55,VAR(14),2,IERR)
      GO TO 50
   30 VAR(15)=VAR(15)-D*VAR(15)
      CALL GWDCS(56,VAR(15),1,IERR)
      GO TO 50
C*****W4 DISTURBANCE
   31 VAR(15)=VAR(15)
      VAR(16)=VAR(16)+D*VAR(16)
      CALL GWBDCS(56,VAR(15),2,IERR)
      GO TO 50
   32 VAR(16)=VAR(16)-D*VAR(16)
      CALL GWDCS(57,VAR(16),1,IERR)
      GO TO 50
C*****WF4 DISTURBANCE
   33 VAR(16)=VAR(16)
      CALL GWDCS(57,VAR(16),1,IERR)
      CALL GSC(0,IERR)
      CALL GSC(1,IERR)
      VAR(17)=D*VAR(17)
      CALL GWJDHS(VAR(17),13,IERR)
      GO TO 55
   34 WF4M=.038795/(.9999995-D)
      IF(VAR(17).LT.WF4M)  GO TO 1000
      CALL GSC(0,IERR)
      CALL GSC(1,IERR)
      VAR(17)=-D*VAR(17)
      CALL GWJDHS(VAR(17),13,IERR)
      GO TO 55
C*****WF7 DISTURBANCE
   35 CALL GSC(0,IERR)
      CALL GSC(1,IERR)
      VAR(17)=.05
      VAR(18)=D
      CALL GWJDHS(VAR(17),13,IERR)
      CALL GWJDHS(VAR(18),14,IERR)
      GO TO 55
   36 IF(VAR(18).LT.D)  GO TO 1000
      CALL GSC(0,IERR)
      CALL GSC(1,IERR)
      VAR(18)=-D
      CALL GWJDHS(VAR(18),14,IERR)
```

```
      GO TO 55
C*****A7 DISTURBANCE
   37 CALL USC(6,1000)
      CALL USC(3,1000)
      VAR(18)=.05
      VAR(19)=-D*VAR(19)
      CALL UNJDMS(VAR(18),14,1000)
      CALL UNJDMS(VAR(19),31,1000)
      GO TO 55
   38 CALL USC(6,1000)
      CALL USC(3,1000)
      VAR(19)=D*VAR(19)
      CALL UNJDMS(VAR(19),31,1000)
      GO TO 55
C*****CIVV DISTURBANCE
   39 CALL USC(6,1000)
      CALL USC(3,1000)
      VAR(19)=.05
      CALL UNJDMS(VAR(19),31,1000)
      IF(VAR(20).LT.-999999.) GO TO 10000
      VAR(20)=-D
      CALL UNJDMS(VAR(20),16,1000)
      GO TO 55
   40 IF(VAR(20).GT.-D) GO TO 10000
      CALL USC(6,1000)
      CALL USC(3,1000)
      VAR(20)=D
      CALL UNJDMS(VAR(20),16,1000)
      GO TO 55
C*****RCVV DISTURBANCE
   41 CALL USC(6,1000)
      CALL USC(3,1000)
      VAR(20)=.05
      CALL UNJDMS(VAR(20),16,1000)
      IF(VAR(21).LT.-999999.) GO TO 10000
      VAR(21)=-D
      CALL UNJDMS(VAR(21),17,1000)
      GO TO 55
   42 IF(VAR(21).GT.-D) GO TO 10000
      CALL USC(6,1000)
      CALL USC(3,1000)
      VAR(21)=D
      CALL UNJDMS(VAR(21),17,1000)
      GO TO 55
   45 CALL USC(6,1000)
      CALL USC(3,1000)
      VAR(21)=.05
      CALL UNJDMS(VAR(21),17,1000)
      CALL USC(2,1000)
      CALL USCOF(1000)
   47 CALL USC(6,1000)
      CALL USC(3,1000)
      GO TO 60
   50 CALL USC(6,1000)
      CALL USC(3,1000)
   55 TYPE 5000,I
      CALL UNCLI(3,INUM,,1000)
   60 RETURN
      END
```

APPENDIX C

F100 SERIES II-3 SYSTEM MATRICES AT VARIOUS POWER CONDITIONS

Full-State System at Sea-Level-Static - Intermediate-Power Condition; Power Lever Angle, 83°

MATRIX A

	1	2	3	4	5	6	7	8
1	-4.721	0.1223	-0.2263	-8629.	-1.598	720.7	-9278.	-95.01
2	-0.1671	-5.230	191.7	-22.44	0.0000	-241.5	-977.6	-3.869
3	0.0000	0.4278D-01	-108.9	0.0000	-1.122	0.4469	0.0000	0.0000
4	0.7904D-03	0.3357D-02	0.1748	-23.32	-0.93549-02	-0.6769	0.2832	0.3552D-02
5	-0.3092D-02	-0.2979D-02	-0.6955D-01	8.360	-256.8	-0.7781E-01	1.939	-0.2535D-01
6	0.3864D-03	0.1168D-02	21.41	1110.	0.7875	-83.61	7.749	0.4087D-01
7	0.1732D-01	-0.2567D-01	0.8527D-02	-0.5360	0.0000	0.3113D-01	-1.359	-0.1628D-01
8	0.2108D-02	-0.1188D-02	0.0000	0.0000	0.0000	0.3113D-01	888.3	-10.51
9	-0.7518D-05	0.9030D-03	-0.860	0.1698	0.5607D-02	0.1285D-01	0.4847D-01	-0.1017D-03
10	0.6325D-03	0.2163D-01	0.194	-0.6832E-01	-0.8898D-02	-0.3113E-03	1.288	0.1017D-01
11	0.1852	0.8753D-02	0.1279	5.360	0.0000	0.1556	722.9	9.635
12	0.7364D-01	0.7466D-02	0.6395D-02	-549.1	-.5610D-01	89.98		
13	-0.7590D-03	0.3581D-03	0.0000	24.85	0.7480D-03	0.6994	0.1550D-01	0.8858D-03
14	0.6755D-05	0.1070D-04	-0.3840D-03	-0.2910D-01	-0.180	0.1402D-02	0.0000	-0.9126D-04
15	0.0000	0.2675D-02	0.0000	12.05	-2972.	0.0000	-8.358	0.0000
16	0.3765D-01	0.2970D-02	0.0000	20.10	0.0000	-0.7781	0.1783 05	115.9

	9	10	11	12	13	14	15	16
1	91.75	-14.73	-0.1104	-910.0	89.65	23.39	0.2971	0.1837
2	-0.2691E 05	-0.1422D 05	-13.54	1.501	26.73	0.0000	0.3917	-0.3627
3	6576.	0.2937D 05	22.94	-1.075	0.0000	0.0000	-0.2029	0.1000
4	97.97	-2.430	-0.2890D-02	0.5376D-01	0.0000	0.5889	-0.1692D-02	0.0000
5	-14.41	0.0000	0.0000	153.7	-2732.	1330.	28.85	0.8859D-01
6	-5821.	-61.82	0.3788	1.833	0.0000	15.70	-0.6756D-01	0.3868
7	0.0000	14.67	0.1088D-01	-0.7367D-01	1.227	0.0000	0.0000	-0.9871
8	17.29	0.333	0.0000	0.5017	3.830	-0.281	-0.5611D-01	-0.1722
9	-101.9	1868.	1.078	0.1795D-02	0.6384D-01	0.0000	0.6768D-03	0.8485D-03
10	-0.1763D-01	-1883.	-1.089	0.7367D-02	0.3830D-01	0.1099	-0.6768D-03	0.5195D-02
11	0.0000	7833.	-14.27	0.3588	0.0000	-7.852	9.9000	0.0000
12	0.322	-3.872	0.2198D-01	-103.5	2268.	-1.570	-23.91	12.19
13	0.5763D-01	-0.2500	-0.1455D-03	-0.4873D-01	0.5107D-01	0.7852D-01	-1.806	0.9971
14	-0.1296	0.1289	0.7022D-04	-0.1611D-02	0.0000	-66.90	1.007	0.7786D-03
15	-329.6	-31.23	0.2335D-01	2071.	18.36	-158.0	4.8566	-0.3898
16	-1045.	173.6	-0.7799D-01	-1954.	-63.88	39.26	2.621	-25.58

MATRIX B

	1	2	3	4	5
1	-78.21	1.889	0.0000	0.0000	0.3991D-02
2	6.539	-262.9	-58.01	-0.3080D-02	0.0000
3	-1.974	0.0000	-16.62	0.2559	-0.1308D-02
4	0.4684D-01	0.2104	0.1396	-0.3675D-04	-0.1087D-04
5	0.3123	-0.9507	-2058.	0.7871D-02	0.1135
6	0.0000	6.312	-5.541	-0.1471D-02	-0.8699D-03
7	0.9367	-0.9110	-1.108	-0.8812D-03	-0.4387D-04
8	0.1249	0.2804	1.108	-0.1471D-02	-0.4387D-03
9	-0.6285D-02	0.8560D-01	0.1394	0.2647D-03	-0.2608D-04
10	0.3787D-02	0.5427	0.1330	0.1176D-04	0.1217D-04
11	0.6285	8.209	0.0000	0.0000	-0.2608D-02
12	-0.3835	0.5062	3.087	-0.2206D-03	-0.1799D-03
13	-0.8996D-02	0.2305D-01	0.1108D-01	0.8239D-05	-0.6956D-05
14	-0.1908D-02	0.3150D-02	-84.06	-0.3284D-05	0.2739D-03
15	0.0000	1.579	-2188.	-0.6617D-02	-0.2918D-02
16	36.35	11.40	-83.11	-0.9991D-02	-0.5892D-03

MATRIX C

	1	2	3	4	5	6	7	8
1	0.1860D-01	-0.6506D-04	0.0000	-0.3031	0.1187D-01	-0.2089D-02	-0.5302D-01	0.0000
2	0.0000	0.7082D-05	-0.1076D-03	-0.1176D-01	-0.8228D-01	0.0000	0.0000	-0.3931D-04
3	0.0000	-0.5703D-02	0.0000	8.576	535.6	0.0000	0.0000	0.0000
4	-0.2412D-03	-0.3601D-03	8.165	-1.717	0.0000	0.0000	0.6200	-0.3251D-02
5	-0.1517D-06	0.6078D-07	-0.5372D-08	-0.2663D-03	-0.2611D-04	-0.3978D-04	-0.2085D-01	-0.1182D-03
6	0.1337D-06	0.0000	-0.1220D-07	0.0000	0.0000	0.0000	-0.9826D-04	-0.9118D-05
7	0.5745D-09	0.4079D-08	0.0000	0.0000	0.0000	0.0000	0.1108D-05	0.1142D-07

	9	10	11	12	13	14	15	16
1	0.0000	0.4485	0.3328D-03	0.1187D-01	0.1021	0.0000	0.1082D-02	0.0000
2	0.0000	0.0000	0.0000	0.0000	0.0000	0.0000	-0.1088D-03	0.0000
3	-136.1	88.44	0.8592D-01	-3.187	0.0000	572.8	0.0000	0.0000
4	-5550.	2.224	0.0000	-0.5726D-01	0.0000	1.258	0.0000	0.2778D-01
5	-0.7365D-03	0.3550D-03	-0.2495D-06	-0.2657D-08	-0.1672D-03	0.5781D-03	-0.5083D-05	0.1762D-02
6	0.0000	0.0000	0.0000	0.0000	0.0000	0.0000	0.0000	0.0000
7	0.0000	-0.2252D-04	-0.1686D-07	0.0000	0.0000	0.0000	0.0000	0.0000

MATRIX D

	1	2	3	4	5
1	0.6894	-0.6738D-01	0.8860D-01	0.0000	0.8173D-04
2	0.0000	1.000	0.0000	0.0000	-0.2065D-08
3	1.998	-2.245	5756.	0.2353D-02	0.6956D-03
4	0.0000	0.0000	-0.8852	-0.2389D-03	0.0000
5	0.0000	0.3479D-04	0.1416D-03	0.0000	-0.2156D-07
6	0.0000	0.0000	0.0000	0.0000	0.0000
7	0.0000	0.0000	0.0000	0.0000	0.0000

Full-State System at Sea-Level-Static Condition; Power Lever Angle, 70°

MATRIX A

	1	2	3	4	5	6	7	8
1	-3.754	-0.2780D-01	-0.1726	-7600.	0.9000	713.9	-2386.	-20.35
2	-0.1495	-3.806	200.7	36.98	-1.690	-237.0	-520.0	-5.218
3	-0.4866D-02	0.1071D-01	-101.0	0.0000	0.0000	1.163	0.0000	0.0000
4	0.7299D-03	0.2526D-02	0.1829	-21.02	-0.3285D-01	-0.7170	0.9801	0.8768D-02
5	-0.6111D-03	0.1071D-02	0.0000	-5.880	-230.9	0.2507	2.179	0.0000
6	0.2758D-01	0.2370D-01	19.13	648.3	0.0000	-75.38	17.02	0.1769
7	0.1557D-01	-0.1984D-01	0.0000	-0.5880	0.0000	0.1038D-01	-6.783	-0.7832D-04
8	0.6488D-03	-0.4990D-03	-0.2168D-01	1.176	0.5025D-01	-0.7772D-01	658.8	-12.98
9	-0.3248D-04	0.5115D-03	-4.483	-0.2352	-0.1405D-01	0.1858D-01	-0.5688D-01	-0.5867D-03
10	0.1194D-02	0.1607D-01	4.300	0.9807D-01	-0.8513D-02	0.3876D-02	0.753	0.8861D-01
11	0.4866D-01	0.0000	0.5420D-01	0.0000	0.0000	-0.1538	222.2	2.273
12	0.6553D-01	0.5052D-02	0.1355D-01	-453.9	0.9025D-01	85.50	1.525	9.423
13	-0.5677D-03	0.2719D-03	0.5821D-03	21.78	-0.9028D-03	0.7368	0.9278D-01	0.6755D-02
14	0.0000	0.2806D-05	0.1220D-03	0.0000	-3.080	0.1308D-02	0.0000	-0.8019D-04
15	0.7297D-02	-0.2865D-02	0.1220	13.23	-2138.	0.0000	-4.901	-0.4913D-01
16	0.0000	0.1559D-02	-0.6778D-01	0.0000	-3.5644	0.2422	9861.	91.29

	9	10	11	12	13	14	15	16
1	-101.7	102.5	0.0000	-588.3	7.183	61.74	-0.3066	3.060
2	-0.2809D 05	-0.1537D 05	-13.47	-1.869	16.16	-17.81	-0.8594	0.7569
3	6882.	0.2439D 05	18.27	0.0000	0.0000	24.63	-0.2203	-0.5807
4	96.21	-0.8020	-0.1138D-02	0.4618D-01	-0.3386	0.2077	0.1869D-02	0.8508D-02
5	-31.96	-8.050	0.0000	167.0	-2268.	1276.	25.19	-0.5867
6	-8120.	16.08	0.3529	2.206	6.762	0.0000	0.7479D-01	-0.1800
7	-3.198	3.220	-0.1128D-02	0.0000	0.6771	1.662	-0.7876D-02	-0.0731
8	31.98	3.220	-0.2277D-02	0.1766	-2.709	-3.328	0.7879D-01	-0.2686
9	-99.00	1356.	0.9431	0.1328D-01	-0.5771D-01	0.2908	0.3788D-03	0.3608D-02
10	-0.7026	-1360.	-0.9459	-0.1501D-01	0.1625	0.3228D-01	-0.4888D-03	0.1802D-02
11	0.0000	8001.	-16.33	0.0000	-6.771	-8.310	0.7876D-01	0.0000
12	-7.986	0.8050	0.2220D-01	-190.1	1883.	-1.287	-20.52	11.68
13	-0.1516	0.1288	0.6831D-04	-0.4963D-01	-0.6771D-01	-0.6609D-01	-0.0558	1.016
14	-0.2156	0.1087	0.7685D-04	0.0000	0.8570D-01	-56.96	1.000	0.9108D-03
15	-71.81	36.20	0.2562D-01	2087.	0.0000	-37.60	-0.1483	-0.8052
16	35.96	301.9	0.0000	-1563.	0.0000	353.2	0.1888	-179.6

MATRIX B

	1	2	3	4	5
1	-77.53	-4.519	33.35	-0.2272D-01	-0.1849D-02
2	-2.614	-182.8	32.92	-0.1345D-01	-0.1815D-02
3	0.0000	2.129	31.43	0.2698	0.1300D-02
4	-0.1560D-01	0.1242	0.1310	0.1071D-03	0.2167D-04
5	0.3122	0.5323	-1771.	0.1071D-02	0.1296
6	-0.6244	2.483	10.47	0.0000	-0.4328D-03
7	0.9989	-0.8871	0.5239	-0.2141D-03	0.4334D-04
8	-0.1249	-0.4968	-2.096	0.4282D-03	0.0000
9	-0.6244D-02	-0.5326D-02	-0.1572	0.3105D-03	-0.8666D-05
10	0.1124D-01	0.7750	0.4191D-01	-0.1285D-04	0.1300D-08
11	0.6244	0.3549	0.0000	-0.2141D-02	-0.2167D-02
12	-0.9366D-01	0.2661	-0.5239	0.2141D-03	0.6501D-04
13	-0.3746D-02	0.1206D-01	0.0000	0.2569D-04	-0.3867D-05
14	0.0000	-0.3194D-02	-68.38	0.0000	0.2730D-03
15	0.0000	-1.597	-1733.	-0.4814D-02	-0.1950D-02
16	0.0000	-0.4440	6.555	0.0000	-0.7585D-02

MATRIX C

	1	2	3	4	5	6	7	8
1	0.1788D-01	0.3993D-04	-0.1735D-02	0.0000	-0.7216D-02	0.0000	-1.290	-0.1294D-01
2	0.1791D-04	0.0000	0.0000	0.0000	0.1011D-02	0.4381D-03	0.4880D-02	0.0000
3	0.5191D-02	0.1996D-02	0.2602	9.407	520.6	-0.6202	-3.486	-0.3458D-01
4	0.2598D-03	0.0000	9.176	0.0000	-0.2166	-0.6200D-01	-0.3489	-0.1089D-01
5	0.2076D-06	-0.1597D-06	-0.2600D-05	0.2820D-03	0.0000	-0.1551D-04	-0.3430D-01	-0.1885D-03
6	0.1355D-06	-0.1190D-06	0.5170D-08	0.0000	-0.4304D-07	0.1848D-07	-0.8871D-04	-0.9131D-06
7	0.3094D-09	0.4164D-08	-0.2068D-07	0.0000	0.0000	0.0000	0.1247D-05	0.1876D-07

	9	10	11	12	13	14	15	16
1	0.0000	-0.7728	0.3644D-03	0.0000	0.0000	-0.2660	0.1196D-02	0.8650D-02
2	0.0000	0.6955D-01	0.4918D-04	-0.1907D-02	-0.1517D-01	-0.1862D-01	0.1675D-03	-0.4037D-03
3	0.0000	-77.28	-0.5464D-01	0.0000	10.83	0.0000	0.0000	0.2884
4	-5801.	0.0000	0.5465D-02	0.0000	1.082	3.990	-0.2392D-01	0.0000
5	-0.2044D-02	-0.2580D-03	-0.2003D-05	-0.4946D-04	0.5418D-03	-0.6650D-03	0.3586D-05	0.2860D-02
6	0.0000	0.0000	0.2171D-08	0.0000	-0.6458D-06	0.0000	0.0000	-0.1719D-07
7	0.1218D-04	-0.2764D-04	-0.1954D-07	0.0000	0.0000	0.0000	0.0000	-0.6975D-07

MATRIX D

	1	2	3	4	5
1	0.9690	0.1703D-01	0.0000	0.0000	-0.1387D-04
2	0.0000	1.000	0.1173D-01	0.0000	0.0000
3	0.9990	-0.5678	3738.	0.0000	0.0000
4	-0.1998	0.0000	0.0000	0.3421D-03	0.1386D-03
5	0.9992D-04	0.0000	0.5031D-03	-0.6861D-07	-0.2773D-07
6	0.5955D-07	0.6768D-07	-0.4996D-06	0.0000	0.4133D-10
7	0.0000	0.1354D-06	0.1998D-05	0.0000	0.0000

Full-State System at Sea-Level-Static Condition; Power Lever Angle, 52°

MATRIX A

	1	2	3	4	5	6	7	8
1	-2.465	-0.6880D-01	0.1448	-2726.	0.5928	585.9	-2013.	-18.84
2	-0.1846	-1.835	192.7	27.88	5.849	-222.5	-652.0	-5.086
3	-0.1058D-01	0.2334D-01	-93.38	0.0000	3.351	1.493	29.56	0.0000
4	0.1764D-02	0.9077D-03	0.1928	-16.07	0.2793D-01	-0.9579	0.9858	0.8758D-02
5	0.1764D-02	0.6483D-03	-0.3812D-01	-3.328	-216.4	-0.1244	0.0000	-0.7007D-01
6	0.5819D-01	-0.7778D-02	18.56	832.0	0.0000	-77.37	17.24	0.1868
7	0.2804D-01	-0.9465D-02	0.6823D-02	0.0000	0.0000	0.0000	-9.858	-0.8875D-01
8	0.2469D-02	-0.2075D-02	0.5459D-01	0.0000	0.1117	0.8976E-01	652.3	-18.20
9	-0.5291D-04	0.7067D-03	-4.575	-0.2662	-0.1117D-01	0.1120D-01	-0.2464D-01	0.2336D-03
10	0.1584D-02	0.8130D-02	4.374	0.1331	0.2234D-02	-0.9952D-03	5.040	0.4638D-01
11	0.4938D-01	0.0000	0.0000	-6.655	-1.117	0.0000	157.7	1.518
12	-0.4665D-01	0.2269D-02	-0.1024D-01	-621.3	-0.5585D-01	58.75	1.878	1.324
13	-0.1577D-02	0.1478D-03	-0.2729D-03	17.36	0.0000	1.000	0.1035	0.9342D-03
14	-0.1984D-04	0.0000	-0.1528D-03	-0.2993D-01	-3.088	0.1119D-02	0.3327D-01	0.0000
15	0.3968D-02	0.0000	0.0000	18.98	-216*.	0.5598	-11.09	-0.1051
16	-0.2204D-02	0.0000	0.0000	-8.317	0.0000	0.3109	9195.	68.89

	9	10	11	12	13	14	15	16
1	114.7	0.0000	0.6503D-01	-608.1	-58.62	9.668	-0.2711	-0.3980
2	-0.2595D 05	-0.1295D 05	-10.32	-1.111	-15.40	0.0000	0.0000	3.896
3	4323.	0.2164D 05	14.82	0.0000	0.0000	-27.33	0.5109	-1.116
4	81.05	0.0000	-0.6126D-03	0.1592	-0.1838	0.2278	0.2128D-02	0.8653D-02
5	-18.01	56.07	0.1225D-01	134.0	-1871.	1075.	22.88	-0.2791
6	-3598.	37.38	0.3064	5.305	14.71	-9.111	0.8515D-01	0.9303
7	-3.602	-1.869	-0.1225D-02	0.0000	-1.471	0.0000	0.8515D-02	-0.9289
8	14.41	3.738	-0.1961D-01	-0.8245	-7.353	1.822	0.1022	-0.1116
9	-65.73	1298.	0.8245	-0.5306D-02	0.7353D-01	-0.5923	0.0000	-0.5582D-02
10	0.3602	-1229.	-0.8288	0.4244D-02	-0.1471	0.5467D-01	0.0000	-0.2977D-02
11	-36.02	8186.	-14.72	0.5306	7.353	9.111	0.8515D-01	0.0000
12	-3.602	-1.869	0.1654D-01	-94.92	1556.	1.822	-18.58	10.31
13	-0.2161	0.0000	0.0000	-0.1634	-0.4412D-01	0.9111D-01	-0.9990	0.9958
14	0.0000	-0.4167D-01	0.2745D-04	0.3582D-02	0.0000	-58.28	0.9959	0.8366D-03
15	0.0000	-42.05	0.0000	2070.	0.0000	-123.0	-0.1016	0.8187
16	0.0000	0.0000	0.1531D-01	-1169.	0.0000	0.0000	0.0000	-291.9

MATRIX B

	1	2	3	4	5
1	-46.62	-3.769	32.51	-0.3207D-02	0.1837D-02
2	-123.5	-148.0	-10.82	-0.6330D-02	-0.4983D-01
3	18.83	1.065	0.0000	0.2811	0.7788D-02
4	-0.1569	0.1332	0.0000	0.0000	-0.3246D-04
5	-1.883	0.0000	-1406.	0.9067D-02	0.1456
6	-16.82	2.486	0.0000	-0.3022D-02	-0.6923D-02
7	0.8785	-0.7457	0.0000	0.3022D-03	0.8654D-04
8	0.2510	-0.4261	1.034	0.1813D-02	0.1731D-03
9	0.1883	-0.1773D-02	-0.7758D-01	0.4585D-03	0.8437D-04
10	0.1757D-01	0.6641	0.6203D-01	-0.2418D-04	0.0000
11	0.0000	0.0000	0.0000	0.0000	-0.4326D-03
12	-0.1882	0.1065	0.0000	-0.1514D-03	-0.6487D-04
13	-0.5020D-02	0.1136D-01	0.1034D-01	0.1813D-04	-0.3462D-05
14	0.2825D-01	-0.8011D-03	-60.96	-0.1359D-04	0.2862D-03
15	-2.824	0.0000	-1454.	-0.6800D-02	-0.9735D-03
16	0.0000	0.4437	6.460	-0.7553D-02	0.0000

MATRIX C

	1	2	3	4	5	6	7	8
1	0.3104D-01	0.0000	-0.2184D-02	0.3195	0.0000	-0.1194D-01	-0.218	-0.3886D-01
2	0.3950D-05	0.2965D-05	-0.1528D-03	-0.1491D-01	0.0000	0.0000	-0.5124D-02	0.0000
3	0.2546D-02	0.0000	-0.2073	20.26	523.7	0.0000	0.0000	-0.7094D-01
4	0.0000	-0.8153D-03	10.27	-2.129	0.2681	0.3975D-01	1.577	0.2990D-01
5	-0.3668D-06	-0.8298D-07	-0.1201D-04	-0.2133D-03	-0.6259D-04	0.1196D-04	-0.4391D-01	-0.2033D-03
6	0.1477D-06	0.0000	-0.1301D-07	0.6348D-06	-0.5327D-07	0.2373D-07	-0.1017D-03	-0.9555D-05
7	0.6409D-09	0.4204D-08	0.0000	0.0000	0.0000	0.0000	0.2588D-05	0.2450D-07

	9	10	11	12	13	14	15	16
1	0.0000	0.0000	0.3922D-03	0.4245D-01	0.0000	0.1457	0.0000	-0.8931D-02
2	-0.1556	-0.4167D-01	0.0000	-0.1188D-02	0.0000	-0.2041D-01	0.0000	0.0000
3	-51.78	53.73	0.3722D-01	0.0000	-10.57	164.7	-0.2596	0.2675
4	-5499.	0.0000	-0.3921D-02	0.0000	-3.530	5.833	-0.1360D-01	0.3870
5	0.2882D-02	-0.1793D-02	-0.1765D-05	0.5940D-04	0.3534D-03	0.1604D-02	-0.1090D-04	0.3376D-02
6	0.0000	0.1782D-05	0.2337D-08	0.5060D-07	-0.7012D-06	-0.8689D-06	0.8121D-08	-0.1774D-07
7	0.0000	-0.2674D-04	-0.1753D-07	0.0000	0.0000	0.0000	0.0000	0.0000

MATRIX D

	1	2	3	4	5
1	0.7631	0.0000	-0.8267D-01	0.1451D-03	-0.4154D-04
2	0.0000	1.000	0.1158D-01	-0.6770D-05	0.0000
3	-5.616	0.0000	2636.	0.4344D-02	-0.1314D-02
4	-10.24	0.5673D-01	-1.656	-0.9669D-03	-0.3734D-02
5	0.1004D-03	0.2272D-04	-0.2480D-03	0.1450D-06	0.1986D-07
6	-0.1197D-06	-0.6773D-07	0.0000	0.2882D-09	0.0000
7	0.0000	0.0000	0.0000	0.0000	0.0000

Full-State System at Sea-Level Static Condition; Power Lever Angle, 36°

MATRIX A

	1	2	3	4	5	6	7	8
1	-2.488	-0.3262D-01	-0.2966	-2556.	2.969	604.3	-1605.	-13.88
2	-0.4666	-3.034	196.4	17.45	-1.463	-281.2	-1339.	-11.38
3	0.6133D-02	0.2196D-01	-90.25	-25.00	0.0000	0.9931	0.0000	0.0000
4	0.1124D-02	0.2013D-02	0.2026	-18.33	0.0000	-1.076	1.858	0.1207D-01
5	-0.3066D-02	0.7316D-03	0.0000	8.332	-249.6	0.1655	1.388	0.8830D-01
6	0.3066D-01	-0.5855D-02	17.98	691.6	0.6991	-79.12	24.92	0.2815
7	0.3169D-01	-0.1727D-01	0.0000	0.8333	0.0000	-0.3310D-01	-17.72	-0.1586
8	0.1636D-02	-0.2342D-02	0.3726D-01	1.667	0.2796	0.1986	725.5	-13.70
9	-0.4089D-04	0.8124D-03	-4.772	-0.2500	-0.3490D-02	0.1821D-01	-0.8307D-01	0.2815D-03
10	0.2887D-02	0.1485D-01	4.556	0.5000D-01	-0.2796D-02	0.8635D-02	8.207	0.6936D-01
11	0.5316D-01	0.0000	0.1863	0.0000	0.0000	0.3310	152.3	1.352
12	-0.1932D-01	0.3513D-02	0.4650D-02	-529.6	-0.1049	57.12	2.358	1.168
13	-0.6256D-03	0.2722D-03	0.5589D-03	19.63	-0.1398D-02	1.109	0.1406	0.1111D-02
14	-0.4599D-05	0.9880D-05	-0.6286D-03	0.1876D-01	-5.359	0.7847D-03	0.0000	-0.2173D-03
15	-0.9202D-02	-0.3295D-02	0.2097	0.0000	-2208.	-0.7887	-6.230	-0.5933D-01
16	.0000	0.0000	0.0000	10.42	-0.8738	0.4139	8667.	58.98

	9	10	11	12	13	14	15	16
1	-238.9	196.0	0.1131	-609.7	-17.89	-10.98	0.2190	-0.6776
2	-0.1839D 05	-2369.	-2.651	0.0000	17.67	-21.67	-0.8320	0.8458
3	3782.	0.1891D 05	11.11	-3.931	-25.30	0.0000	0.3098	-0.6384
4	83.30	-9.812	-0.4997D-02	0.4586	0.0000	0.0000	-0.7736D-02	0.0000
5	0.0000	0.0000	-0.1332D-01	129.7	-1687.	1097.	19.94	-0.3192
6	-3867.	-184.7	0.1466	15.72	8.435	0.0000	0.1031	0.0000
7	-4.503	57.72	0.3198D-01	0.0000	0.8435	-1.035	0.0000	-0.9769
8	0.0000	9.235	-0.2665D-02	0.1310	0.0000	6.209	-0.2063D-01	-0.3805
9	-86.00	1245.	0.6783	0.3270D-02	-0.4211D-01	0.5182D-01	0.1586D-02	0.0000
10	0.9006D-01	-1295.	-0.7073	-0.1179D-01	0.1518	-0.1242	0.1238D-02	0.3805D-02
11	-95.03	8727.	-15.03	0.0000	8.438	-10.35	0.0000	0.0000
12	0.0000	-13.85	0.3320D-02	-103.8	1808.	0.0000	-16.90	10.28
13	0.0000	-0.6926	-0.5330D-03	-0.4926	0.3374D-01	-0.6209D-01	-0.5875	0.9976
14	-0.2027	0.1559	-0.5996D-04	-0.7371D-02	-0.5694D-01	-48.98	0.9981	0.5578D-03
15	0.0000	155.9	0.0000	2040.	18.99	93.13	-0.8640	0.4787
16	56.29	0.0000	0.0000	-892.6	0.0000	-12.93	0.1289	-348.5

MATRIX B

	1	2	3	4	5
1	-22.73	-1.507	-5.475	-0.2323D-01	0.9202D-03
2	39.58	-133.8	10.81	-0.1833D-01	0.1361D-01
3	-3.780	0.0000	15.48	0.2889	-0.1300D-02
4	0.9452D-01	0.1242	-0.1290	0.0000	0.2167D-04
5	-0.6299	-0.1774	-1030.	0.2188D-02	0.1766
6	7.560	2.129	-5.161	0.0000	0.2167D-02
7	0.3780	-0.7453	0.0000	0.4377D-03	0.0000
8	-0.7560	-0.2129	-2.064	-0.1751D-02	-0.8668D-04
9	-0.3151D-01	0.1777D-02	0.0000	0.3720D-03	-0.2170D-05
10	-0.1260D-01	0.6182	-0.5161D-01	-0.6127D-04	0.4334D-05
11	-2.520	-0.7098	10.32	0.0000	-0.8667D-03
12	-0.1891	0.2129	0.2585	-0.6562D-03	-0.4334D-04
13	-0.2772D-01	0.9938D-02	0.1032D-01	0.2625D-04	-0.3467D-05
14	0.8506D-02	-0.7990D-03	-51.66	-0.9853D-05	0.2789D-03
15	2.837	0.7990	-1103.	0.9853D-02	0.9756D-03
16	6.300	0.0000	0.0000	0.0000	0.2167D-02

MATRIX C

	1	2	3	4	5	6	7	8
1	0.3670D-01	-0.2344D-04	-0.1489D-02	0.1335	0.0000	0.1060D-01	-9.216	-0.7689D-01
2	0.1963D-04	-0.2343D-05	-0.4471D-03	0.4000D-01	0.0000	0.1059D-02	0.0000	0.0000
3	-0.3271D-02	0.0000	-0.2678	11.98	629.2	-0.9517	-4.431	-0.3872D-01
4	-0.3274D-03	-0.7027D-03	12.80	0.0000	-0.2237	-0.5302D-01	0.8828	0.0000
5	0.9827D-07	-0.2331D-07	0.8936D-05	0.0000	-0.7834D-04	-0.2118D-04	-0.5503D-01	-0.2353D-03
6	0.1924D-06	-0.4188D-09	-0.8883D-08	-0.7947D-06	-0.6667D-07	-0.1263D-06	-0.1305D-03	-0.1110D-05
7	0.1365D-08	0.4886D-08	0.0000	0.0000	0.0000	0.0000	0.2377D-05	0.2073D-07

	9	10	11	12	13	14	15	16
1	0.0000	0.0000	0.2134D-03	0.0000	0.2699	-0.8967	-0.3299D-02	0.0000
2	-0.7208D-01	0.0000	0.0000	0.0000	0.1350D-01	0.0000	0.0000	0.0000
3	64.73	0.0000	0.0000	0.9817	25.62	-86.31	-0.1883	0.0000
4	-6131.	-3.698	0.0000	-0.1089	-1.351	-1.657	-0.8951D-01	-0.3800D-01
5	-0.2160D-02	-0.5542D-02	0.6393D-06	-0.8391D-08	-0.8100D-03	0.0000	-0.8252D-05	0.8158D-02
6	0.4294D-05	-0.2202D-05	-0.2542D-08	0.0000	-0.2413D-05	-0.1578D-05	0.1967D-07	0.6088D-0
7	0.00000	-0.3743D-04	-0.2161D-07	0.0000	0.0000	0.0000	0.0000	0.0000

MATRIX D

	1	2	3	4	5
1	0.4032	0.5675D-02	0.0000	0.0000	-0.6981D-05
2	0.0000	1.000	-0.2477D-01	0.1800D-04	-0.1387D-05
3	0.0000	-0.5102	1556.	0.0000	0.0000
4	4.239	0.5670D-01	-2.478	-0.1800D-02	0.1664D-02
5	-0.3227D-03	-0.5680D-04	0.9513D-03	0.3502D-06	-0.1110D-06
6	0.3605D-06	0.0000	-0.1477D-05	-0.2504D-08	0.0000
7	0.0000	0.0000	0.0000	0.0000	0.0000

Seventh-Order System at Sea-Level-Static - Intermediate-Power Condition
Power Lever Angle, 83°

MATRIX $\bar{A}_s$

	1	2	3	4	5	6	7
1	-4.722	0.1261	-0.8135	11.59	-701.6	880.8	-527.6
2	-0.3838	-10.65	191.7	0.7686D-01	158.9	-285.8	-287.0
3	0.5965D-01	1.749	-35.10	-0.9937D-02	-27.30	1.043	50.88
4	-0.7693	-40.55	663.9	-58.78	823.0	-125.0	-787.0
5	0.6208D-01	-0.1598	1.596	0.1091	-1712.	38.20	1877.
6	0.8268D-02	-1.125	31.36	-1.889	5.868	-52.33	-10.69
7	0.9009D-01	-0.9306D-01	-0.1998	0.8158D-02	898.8	-1.003	-860.2

MATRIX $\bar{B}_s$

	1	2	3	4	5
1	-75.73	2.830	-696.8	-0.2319D-02	0.3385D-02
2	5.136	-502.9	27.63	0.2196D-01	0.8123D-02
3	-1.538	75.31	-22.72	0.2501	-0.2288D-02
4	-36.16	-1697.	-362.9	0.1751	0.2097D-01
5	12.35	2.814	-3731.	-0.1089D-01	0.6110D-01
6	-0.2075D-01	-43.18	-13.50	0.3753D-02	-0.6767D-03
7	1.441	-5.879	501.8	0.9686D-03	-0.5071D-03

MATRIX $\bar{C}_s$

	1	2	3	4	5	6	7
1	0.1859D-01	-0.1065D-03	0.6609D-03	0.3532D-03	-0.1099	-0.1059D-01	0.1167
2	-0.1122D-06	0.9137D-05	-0.2006D-03	0.2101D-08	0.1201D-01	-0.5784D-03	-0.1278D-01
3	-0.1896D-01	-0.4289D-01	0.8850	-0.3805	858.9	-1.552	100.1
4	-0.2919D-01	-1.075	17.19	0.1588D-01	26.33	-0.8305	-36.14
5	0.2416D-05	-0.1636D-04	0.1588D-03	-0.2562D-05	-0.1538	0.3228D-03	0.1818
6	0.1337D-06	-0.9095D-11	-0.1213D-07	-0.6653D-11	-0.8186D-07	0.1318D-09	-0.1509D-08
7	0.5619D-09	0.3750D-08	-0.6389D-07	-0.7340D-13	0.6593D-08	0.3306D-10	0.1882D-06

MATRIX $\bar{D}_s$

	1	2	3	4	5
1	0.6905	-0.6711D-01	-0.3858D-01	-0.9737D-06	0.8183D-08
2	-0.1020D-03	1.0000	0.1332D-01	0.9670D-07	-0.2874D-05
3	2.858	-3.175	5766.	0.1881D-02	-0.2061D-01
4	-0.2215	-47.82	11.86	0.4924D-02	0.7511D-03
5	0.1225D-02	0.2638D-03	-0.1595	-0.1101D-05	0.3752D-07
6	0.6005D-10	-0.8490D-09	-0.8354D-07	0.2859D-11	0.8353D-12
7	-0.1201D-09	-0.1986D-07	0.8484D-08	-0.1830D-12	-0.8934D-13

MATRIX $\bar{H}_s$

	1	2	3	4	5	6	7
1	1.000	0.0000	0.0000	0.0000	0.0000	0.0000	0.0000
2	0.0000	1.000	0.0000	0.0000	0.0000	0.0000	0.0000
3	0.0000	0.0000	1.000	0.0000	0.0000	0.0000	0.0000
4	0.0000	0.0000	0.0000	1.000	0.0000	0.0000	0.0000
5	0.0000	0.0000	0.0000	0.0000	1.000	0.0000	0.0000
6	0.0000	0.0000	0.0000	0.0000	0.0000	1.000	0.0000
7	0.0000	0.0000	0.0000	0.0000	0.0000	0.0000	1.000
8	0.9825D-04	0.2172D-03	-0.1596D-02	0.1589D-03	0.9998	-0.3147D-02	7.006
9	-0.2913D-01	-1.082	17.30	0.1446D-01	29.21	-0.7879	-38.97
10	0.1733D-03	0.4969D-02	0.9638	0.1744L-05	-0.9705D-01	-0.5375D-03	0.1650
11	0.9434D-02	0.5942D-02	1.110	-0.1225D-03	-0.1726D-01	0.1601D-01	6.556
12	-0.2088D-05	0.9858D-05	-0.7331D-04	-0.2586D-04	1.043	-0.7256D-03	0.9152D-02
13	0.1946D-01	0.2776D-01	-0.2613	0.4135	268.2	-0.6523	-242.8
14	0.2363D-01	0.1440D-01	-0.1491	0.4231	136.7	2.289	-129.7
15	0.6951D-03	-0.8835D-02	0.8871D-01	-0.3447D-01	-86.83	1.579	81.42
16	0.1466D-02	-0.9275D-02	0.9025D-01	-0.1638D-02	-87.55	0.1958	82.13

MATRIX $\bar{H}_u$

	1	2	3	4	5
1	0.0000	0.0000	0.0000	0.0000	0.0000
2	0.0000	0.0000	0.0000	0.0000	0.0000
3	0.0000	0.0000	0.0000	0.0000	0.0000
4	0.0000	0.0000	0.0000	0.0000	0.0000
5	0.0000	0.0000	0.0000	0.0000	0.0000
6	0.0000	0.0000	0.0000	0.0000	0.0000
7	0.0000	0.0000	0.0000	0.0000	0.0000
8	0.1434D-02	-0.2028D-01	-1.040	0.6828D-04	0.1040D-04
9	0.2484	87.75	-15.01	-0.5214D-02	-0.8035D-03
10	-0.1750D-02	-0.2177	0.6502D-01	-0.1983D-05	-0.1535D-05
11	-0.3245D-01	-0.4592	0.4581D-01	-0.1761D-05	0.1132D-03
12	-0.7673D-04	0.2140D-03	-1.043	-0.3037D-05	0.1551D-05
13	2.138	0.3724	-278.8	-0.1741D-02	0.1218D-03
14	1.111	0.2730	16.82	-0.1281D-02	-0.2739D-01
15	-0.6864	-0.1555	90.15	0.6089D-03	-0.3647D-04
16	-0.6974	-0.1326	90.93	0.6228D-03	-0.4675D-04

DEFINE XT = TRANSPOSE OF VECTOR X
THE SYSTEM STATES ARE: XT = (NL,NH,P4,T41,P7,P41,P13)

Fifth-Order System at Sea-Level-Static - Intermediate-Power Condition
Power Lever Angle, 83°

MATRIX $\bar{A}_c$

	1	2	3	4	5
1	-4.769	-10.11	288.8	-2.136	-1313.
2	-0.4289	-5.338	44.87	7.050	-124.2
3	0.6971D-01	1.719	-34.56	-0.3558D-01	26.61
4	-0.9301	-37.75	590.3	-51.24	-357.5
5	0.3553	-1.209	21.93	-0.8603	-147.3

MATRIX $\bar{B}_c$

	1	2	3	4	5
1	-77.89	-387.0	-1503.	0.3094D-01	-0.2160D-02
2	4.492	-297.7	-167.1	0.3873D-02	0.7556D-02
3	-1.380	73.89	32.22	0.2502	-0.2316D-02
4	-40.37	-1586.	-1117.	0.1647	0.2336D-01
5	16.94	-44.80	-2139.	-0.4886D-02	0.5903D-01

MATRIX $\bar{C}_s$

	1	2	3	4	5
1	0.1862D-01	0.1025D-03	-0.5889D-02	0.6638D-03	0.1522D-01
2	-0.2671D-05	0.2345D-04	-0.5230D-03	0.3636D-04	-0.1868D-02
3	0.4193D-03	-0.2513D-01	-0.6200	-0.2883	561.4
4	-0.3636D-01	-1.051	16.75	0.3664D-01	-12.00
5	0.3010D-04	-0.4527D-04	0.1022D-03	-0.4549D-06	-0.3576D-02
6	0.1308D-06	0.2334D-08	0.1422D-07	-0.1216D-08	-0.1608D-04
7	0.5979D-09	0.3721D-08	-0.6419D-07	0.1370D-10	0.2022D-06

MATRIX $\overline{D}_s$

	1	2	3	4	5
1	0.6909	-0.5969D-01	0.9375D-01	-0.1501D-05	0.4184D-04
2	-0.1413D-03	1.001	-0.2960D-03	0.3088D-07	-0.2853D-05
3	3.173	-2.998	5876.	0.1566D-02	-0.2069D-01
4	-0.3339	-46.34	-27.58	0.4794D-02	0.8005D-03
5	0.1668D-02	-0.1555D-02	-0.5395D-02	-0.8022D-06	-0.1185D-06
6	-0.4723D-07	0.1648D-06	-0.1650D-04	-0.2655D-10	0.1664D-10
7	0.4570D-09	-0.1651D-07	0.2053D-06	0.2184D-12	-0.2876D-12

MATRIX $\overline{H}_s$

	1	2	3	4	5
1	1.000	0.0000	0.0000	0.0000	0.0000
2	0.0000	1.000	0.0000	0.0000	0.0000
3	0.0000	0.0000	1.000	0.0000	0.0000
4	0.0000	0.0000	0.0000	1.000	0.0000
5	0.0000	0.0000	0.0000	0.0000	1.000
6	0.1181D-03	-0.2146D-01	0.5996	-0.2847D-01	-0.1050
7	0.1955D-03	-0.1554D-03	-0.1741D-02	0.7988D-04	1.062
8	0.1468D-02	-0.8041D-03	-0.1568D-01	0.8081D-03	8.443
9	-0.3684D-01	-1.059	16.89	0.3378D-01	-12.10
10	0.2055D-03	0.4954D-02	0.9628	0.3022D-04	0.7826D-01
11	0.1072D-01	0.4577D-02	1.108	-0.5376D-04	6.957
12	-0.3837D-06	0.2401D-04	-0.5243D-03	-0.4476D-05	1.053
13	-0.2801D-01	0.7943D-01	-0.2305	0.4128	10.72
14	-0.1403D-02	-0.1457D-01	1.449	0.3476	-1.304
15	0.1680D-01	-0.5539D-01	0.8930	-0.7292D-01	-0.4927
16	0.1755D-01	-0.2624D-01	0.6467D-01	-0.6498D-03	-0.3110

MATRIX $\overline{H}_u$

	1	2	3	4	5
1	0.0000	0.0000	0.0000	0.0000	0.0000
2	0.0000	0.0000	0.0000	0.0000	0.0000
3	0.0000	0.0000	0.0000	0.0000	0.0000
4	0.0000	0.0000	0.0000	0.0000	0.0000
5	0.0000	0.0000	0.0000	0.0000	0.0000
6	0.1037D-02	0.8221	0.4809	-0.7132D-04	0.1271D-04
7	-0.3134D-02	0.1098D-01	-1.091	-0.1949D-05	0.1074D-05
8	-0.2052D-01	0.5407D-01	-8.681	0.5485D-04	0.1788D-04
9	0.3657	46.68	27.11	-0.5082D-02	-0.9553D-03
10	-0.2268D-02	-0.2163	-0.1151	-0.2266D-05	-0.1365D-05
11	-0.5301D-01	-0.3739	-7.107	-0.1570D-04	0.1205D-03
12	-0.1062D-03	-0.2820D-03	-1.053	-0.3003D-05	0.1552D-05
13	2.897	-2.826	-14.83	-0.1222D-02	-0.1469D-03
14	1.520	0.7307	159.3	-0.1192D-02	-0.2750D-01
15	-0.9399	2.037	2.123	0.3375D-03	0.7106D-04
16	-0.9546	0.9303	1.455	0.4488D-03	0.4396D-04

DEFINE XT = TRANSPOSE OF VECTOR X
XT = (NL,NH,P4,T41,P7)

Third-Order System at Sea-Level-Static - Intermediate-Power Condition; Power Lever Angle, 83°

MATRIX $\overline{A}_s$

	1	2	3
1	-8.137	-3.252	153.8
2	-1.012	-9.822	111.3
3	0.1409	1.636	-32.68

MATRIX $\overline{B}_s$

	1	2	3	4	5
1	-239.0	-153.9	0.1802D 05	0.9437D-01	-0.5818
2	-22.68	-493.6	2281.	0.3593D-01	-0.6119D-01
3	1.997	71.54	-370.1	0.2487	0.8816D-02

MATRIX $\overline{C}_s$

	1	2	3
1	0.1863D-01	-0.4297D-03	0.2659D-02
2	-0.7851D-05	0.3679D-05	-0.2507D-03
3	1.485	-2.107	43.95
4	-0.6920D-01	-1.029	16.13
5	0.2073D-04	-0.3038D-04	-0.2070D-03
6	0.8860D-07	0.6867D-07	-0.1367D-05
7	0.1128D-08	0.2887D-08	-0.4683D-07

MATRIX $\overline{D}_s$

	1	2	3	4	5
1	0.6917	-0.8159D-01	-0.7964D-01	0.5966D-07	0.4654D-04
2	-0.3847D-03	0.9997	0.2475D-01	0.2410D-06	-0.3551D-05
3	71.66	-66.58	-2574.	-0.2988D-01	0.2130
4	-1.891	-45.89	155.6	0.5576D-02	-0.4270D-02
5	0.1223D-02	-0.1081D-02	0.4624D-01	-0.6102D-06	-0.1602D-05
6	-0.2050D-05	0.2270D-05	0.2247D-03	0.8399D-09	-0.6653D-08
7	0.2566D-07	-0.4295D-07	-0.2829D-05	-0.1069D-10	0.8363D-10

MATRIX $\overline{H}_s$

	1	2	3
1	1.000	0.0000	0.0000
2	0.0000	1.000	0.0000
3	0.0000	0.0000	1.000
4	-0.3647D-01	-0.7083	10.93
5	0.2626D-02	-0.4073D-02	0.8508D-01
6	0.8807D-03	-0.8722D-03	0.2796
7	0.2982D-02	-0.4539D-02	0.8953D-01
8	0.2361D-01	-0.3577D-01	0.7115
9	-0.6986D-01	-1.033	16.23
10	0.4098D-03	0.4614D-02	0.9698
11	0.2899D-01	-0.2372D-01	1.700
12	0.2764D-02	-0.4261D-02	0.8900D-01
13	-0.1491D-01	-0.2566	5.192
14	-0.1750D-01	-0.2554	5.136
15	0.1817D-01	-0.1728D-02	0.5526D-01
16	0.1675D-01	-0.2451D-01	0.3111D-01

MATRIX $\overline{H}_u$

	1	2	3	4	5
1	0.0000	0.0000	0.0000	0.0000	0.0000
2	0.0000	0.0000	0.0000	0.0000	0.0000
3	0.0000	0.0000	0.0000	0.0000	0.0000
4	1.658	30.05	-82.91	-0.3593D-02	0.2440D-02
5	-0.1247	0.1287	15.01	0.5417D-04	-0.4151D-03
6	-0.3307D-01	-0.4679D-01	1.265	0.2528D-04	-0.1318D-04
7	-0.1355	0.1501	14.85	0.5532D-04	-0.4397D-03
8	-1.072	1.165	119.0	0.5093D-03	-0.3985D-02
9	1.931	46.13	-157.4	-0.5859D-02	0.4252D-02
10	-0.1198D-01	-0.2054	1.057	0.1864D-05	-0.3378D-04
11	-0.9207	0.5198	97.31	0.3613D-03	-0.2767D-02
12	-0.1314	0.1351	14.75	0.5404D-04	-0.4355D-03
13	2.248	10.96	111.9	-0.2125D-02	-0.3591D-02
14	2.259	11.01	110.9	-0.2511D-02	-0.2612D-01
15	-0.9993	-0.2176	0.7786	0.5729D-03	0.9761D-04
16	-0.9169	0.8707	-3.160	0.4383D-03	0.1715D-03

DEFINE XT = TRANSPOSE OF VECTOR X
THE SYSTEM STATES ARE: XT = (NL,NH,P4)

REFERENCES

1. Szuch, John R.; and Seldner, Kurt: Real Time Simulation of F100-PW-100 Turbofan Engine Using Hybrid Computer. NASA TM X-3261, 1975.

2. Szuch, John R.; Seldner, Kurt; and Cwynar, David S.: Development and Verification of Real-Time Hybrid Computer Simulation of F100-PW-100(3) Turbofan Engine. NASA TP-1034, 1977.

3. Ogata, Katsuhiko: State Space Analysis of Control Systems. Prentice Hall, Inc., 1967.

4. Blackburn, Thomas R.; and Vaughan, David R.: Application of Linear Optimal Control and Filtering Theory to the SATURN V Launch Vehicle. IEEE Trans. Automat. Contr., vol. AC-16, no. 6, Dec. 1971, pp. 799-806.

5. Weinberg, Marc S.: Low Order Linearized Models of Turbine Engines. ASD-Tr-75-24, Wright-Patterson AFB, 1975. (AD-A18841.)

6. Seldner, Kurt: Simulation of a Turbofan Engine for Evaluation of Multivariable Optimal Control Concepts. NASA TM X-71912, 1976.

TABLE I. - EIGENVALUES FOR FULL STATE LINEAR MODELS AT SEA LEVEL STATIC AND VARIOUS POWER CONDITIONS

Power lever angle, deg	Eigenvalue, rad/sec	Power lever angle, deg	Eigenvalue, rad/sec
83	-4.86 -6.49 -15.22±j10.75 -20.74 -37.02±j8.79 -89.3±j40.36 -125±j55.31 -49.4±j124.8 -38.1±j333.9 -1542.6	52	-1.86 -3.36 -15.9±j7.24 -20.7 -26.48 -45.62 -47.44±j38.05 -98.91±j42.05 -194.38±j27.5 -54.14±j287.94 -1353.1
70	-4.3±j1.30 -14.91±j8.60 -20.77 -31.22 -42.25 -62.58±j49.61 -102.85±j48.91 -140.95±j84.05 -51.24±j312.73 -1415.7	36	-2.17±j0.95 -19.05±j8.79 -20.26 -29.01 -47.34 -47.55±j40.39 -107.38±j45.18 -160.59 -292.9 -62.13±j262.21 -1344.9

TABLE II. - EIGENVALUES FOR FULL-STATE AND REDUCED-ORDER LINEAR MODELS AT SEA LEVEL STATIC INTERMEDIATE POWER CONDITION

[Power lever angle, 83°.]

Linear model	Eigenvalue, rad/sec	Linear model	Eigenvalue, rad/sec
Full state (16th order)	-4.86 -6.49 -15.22±j10.75 -20.74 -37.02±j8.79 -89.3±j40.36 -125±j55.31 -49.4±j124.8 -38.1±j333.9 -1542.6	7th order	-49.3 -73.1 -2141
		5th order	-4.25 -6.85 -38.84±j16.95 -154.4
7th order	-4.80 -7.52 -22.4 -31.1	3rd order	-4.24 -6.61 -39.8

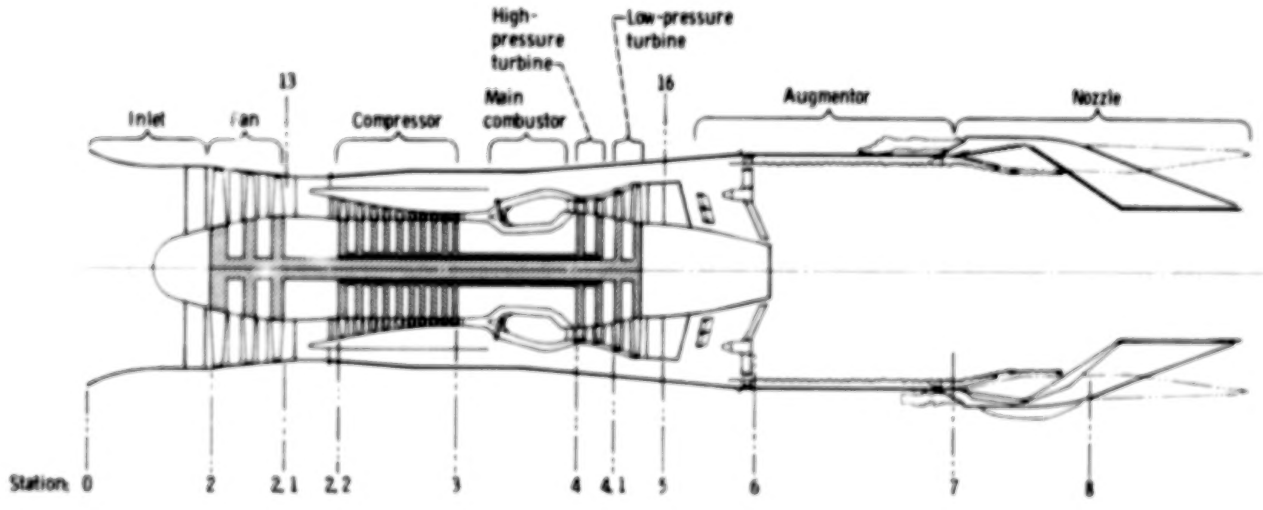

Figure 1. - Schematic representation of F100-PW-100(3) augmented turbofan engine.

CD-11819-07

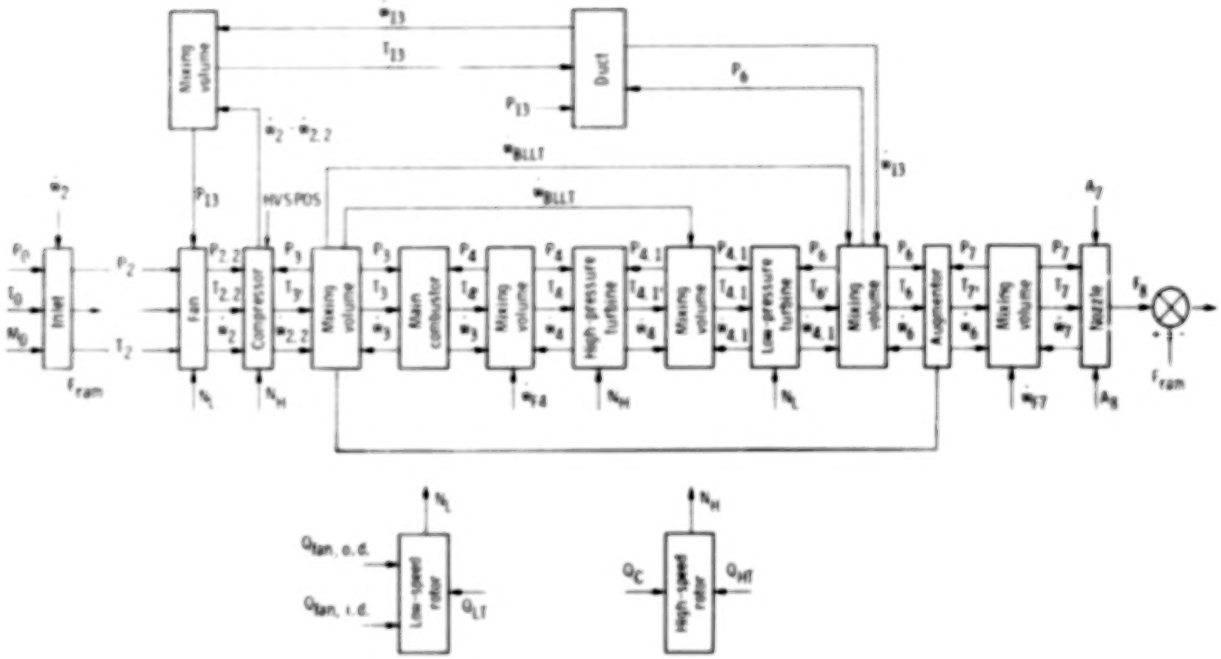

Figure 2. - Computational flow diagram of real-time F100-PW-100 engine simulation.

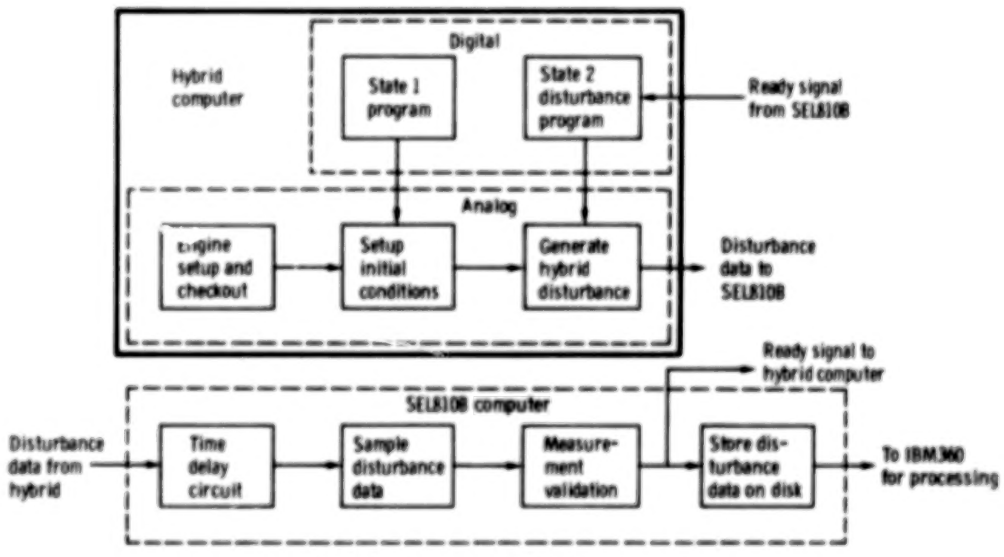

Figure 3. - Generation of data for linear models.

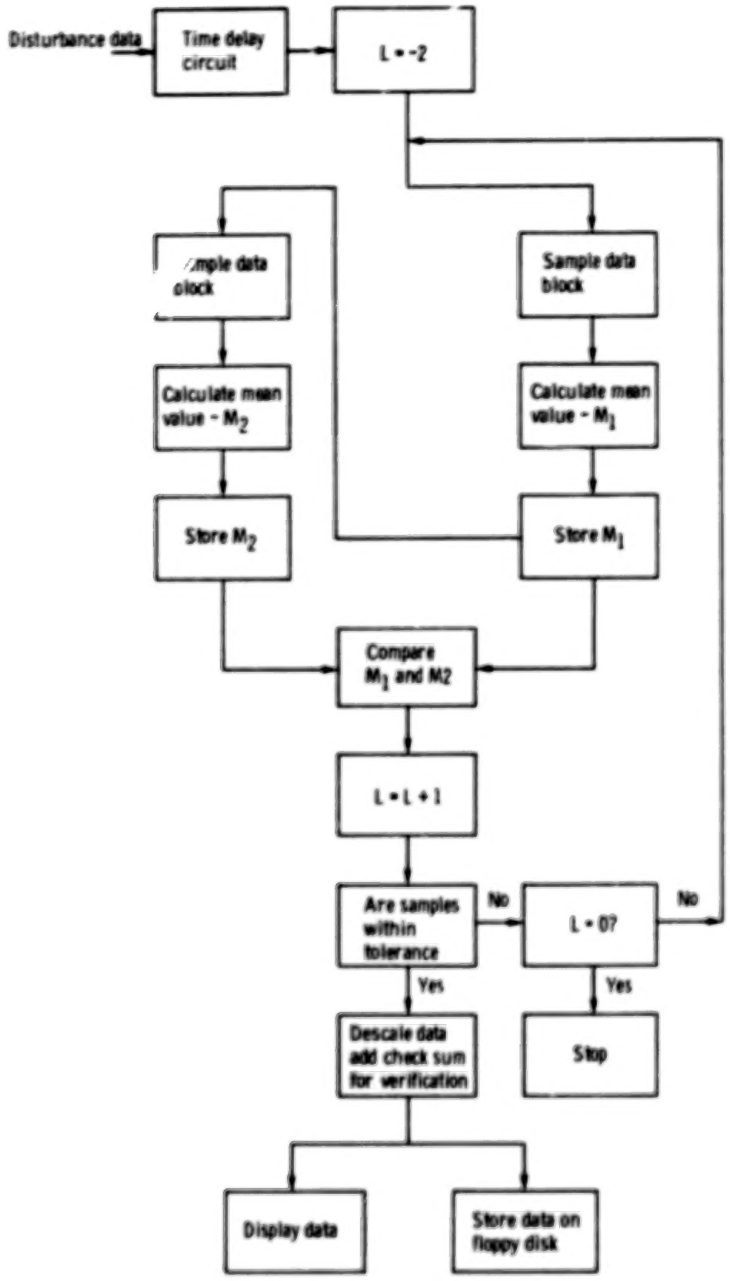

Figure 4. - Sampling and recording processes for state variable disturbance data (SEL810B computer).

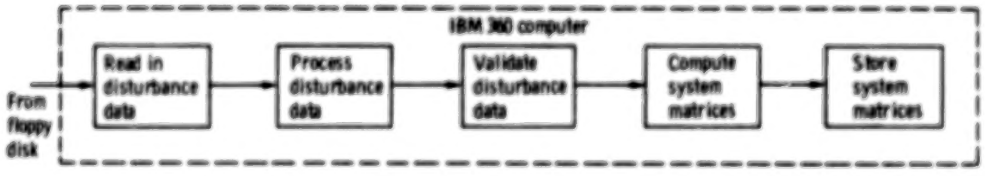

Figure 5. - Data verification, processing, and linear model generation.

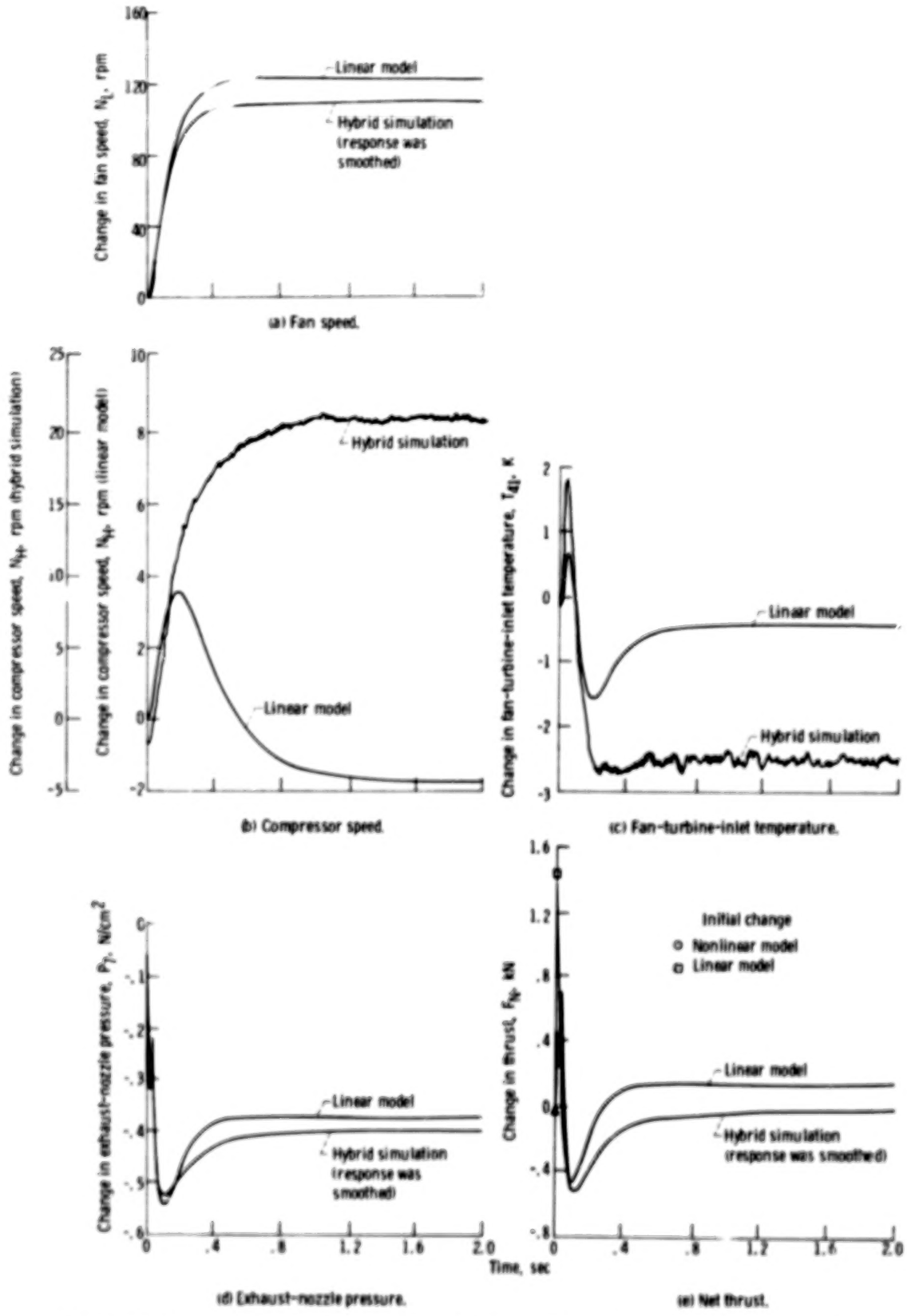

Figure 6. - Comparison of transient response of nonlinear hybrid simulation and full-state model for step change in exhaust-nozzle area. Sea-level-static - intermediate-power condition.

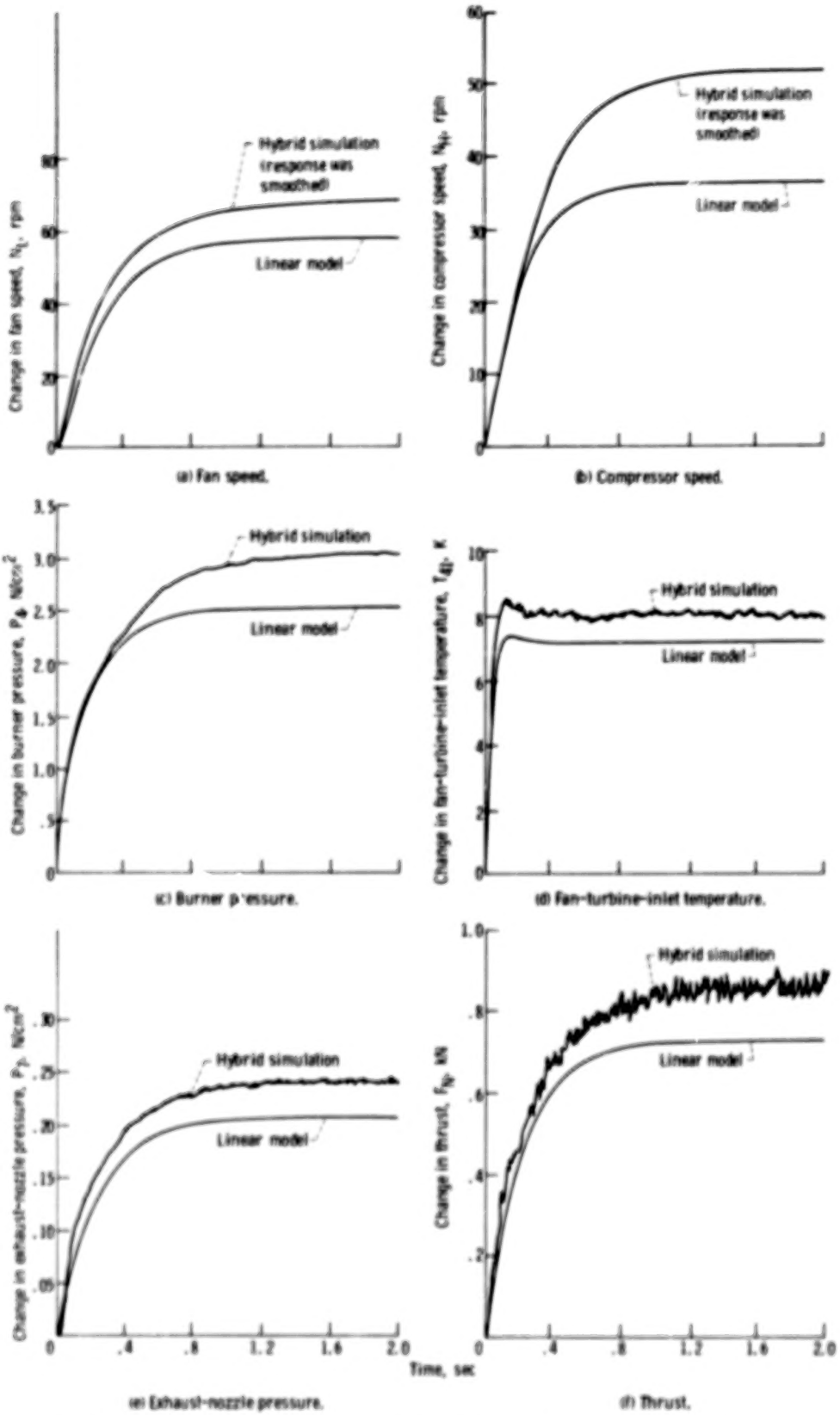

Figure 7. - Comparison of transient response of nonlinear hybrid simulation and full-state model for step change in fuel flow. Sea-level-static - intermediate-power condition.

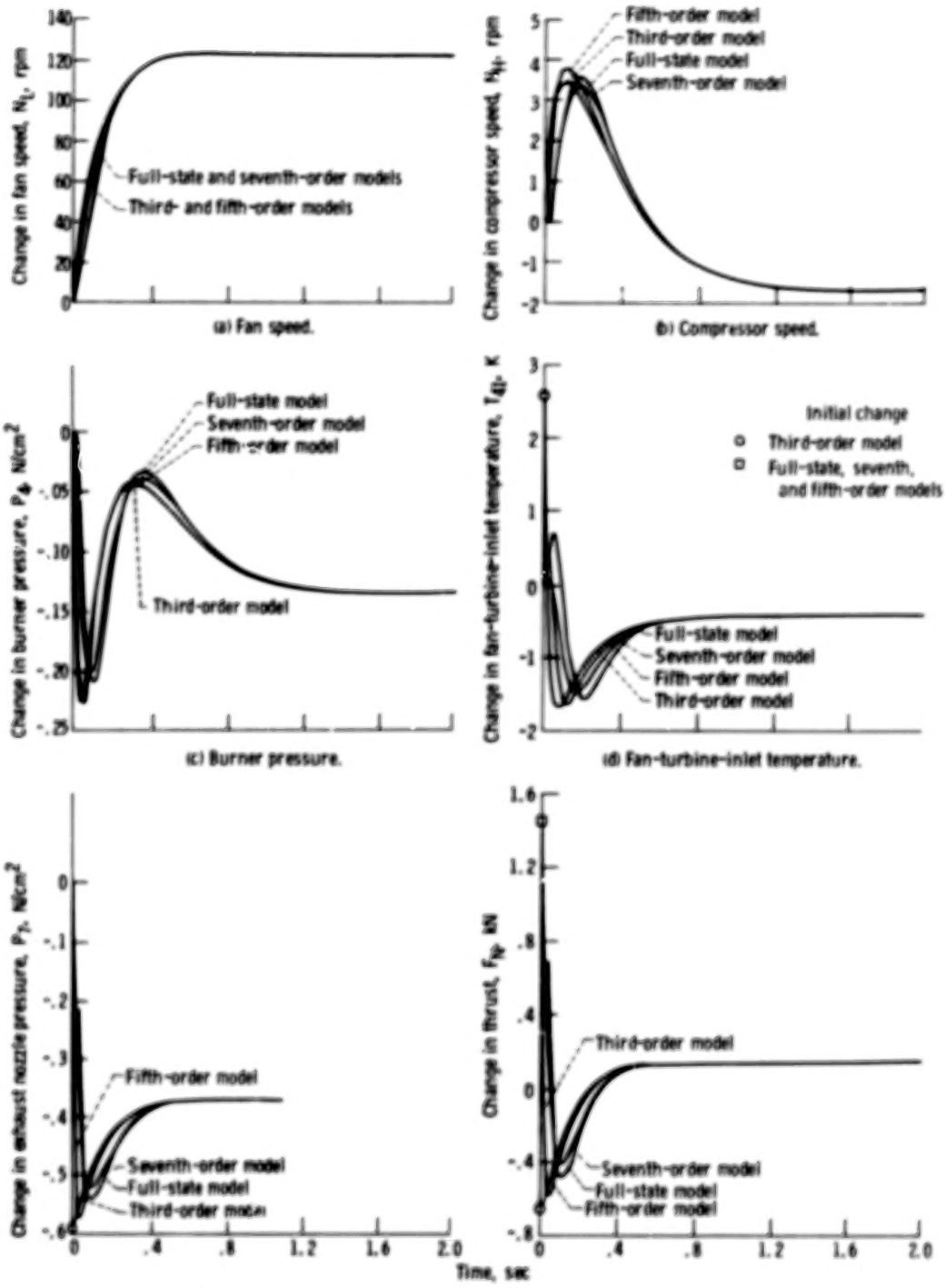

Figure 8. - Comparison of linear models for step change in exhaust nozzle area. Sea-level-static - intermediate-power condition.

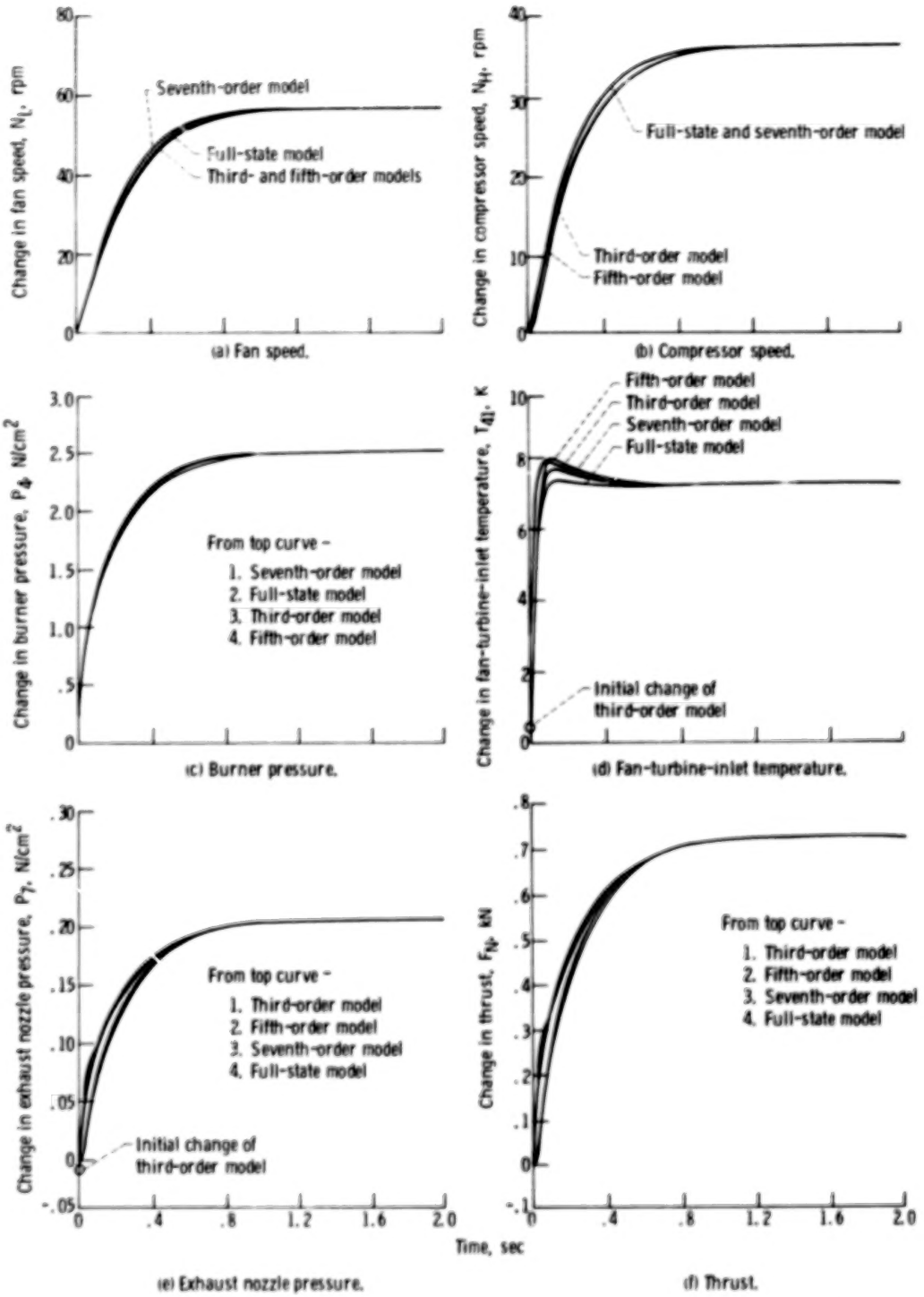

Figure 9. - Comparison of linear models for step change in main burner fuel flow. Sea-level-static - intermediate-power condition.

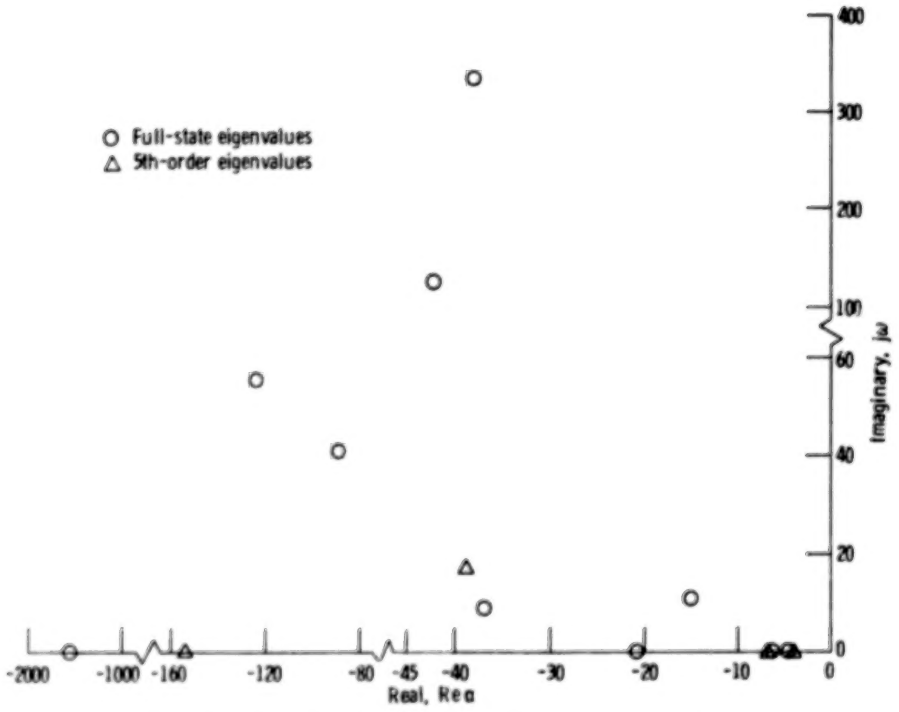

Figure 10. - Eigenvalues for full-state and fifth-order linear models.

1. Report No.	2. Government Accession No.	3. Recipient's Catalog No.
NASA TP-1261		

4. Title and Subtitle	5. Report Date
PROCEDURES FOR GENERATION AND REDUCTION OF LINEAR MODELS OF A TURBOFAN ENGINE	August 1978
	6. Performing Organization Code

7. Author(s)	8. Performing Organization Report No.
Kurt Seldner and David S. Cwynar	E-9460
	10. Work Unit No.
	505-05

9. Performing Organization Name and Address	11. Contract or Grant No.
National Aeronautics and Space Administration Lewis Research Center Cleveland, Ohio 44135	
	13. Type of Report and Period Covered
	Technical Paper

12. Sponsoring Agency Name and Address	14. Sponsoring Agency Code
National Aeronautics and Space Administration Washington, D.C. 20546	

15. Supplementary Notes

16. Abstract

A real-time hybrid simulation of the Pratt & Whitney F100-PW-F100 turbofan engine was used for linear-model generation. The linear models were used to analyze the effect of disturbances about an operating point on the dynamic performance of the engine. A procedure that disturbs, samples, and records the state and control variables was developed. For large systems, such as the F100 engine, the state vector is large and may contain high-frequency information not required for control. Thus, reducing the full-state to a reduced-order model may be a practicable approach to simplifying the control design. A reduction technique was developed to generate reduced-order models. Selected linear and nonlinear output responses to exhaust-nozzle area and main-burner-fuel-flow disturbances are presented for comparison.

17. Key Words (Suggested by Author(s))	18. Distribution Statement
Turbofan engines Computerized simulation Mathematical models	Unclassified - unlimited STAR Category 66

19. Security Classif. (of this report)	20. Security Classif. (of this page)	21. No. of Pages	22. Price*
Unclassified	Unclassified	43	A03

* For sale by the National Technical Information Service, Springfield, Virginia 22161

NASA-Langley, 1978